It's getting hot in here – Microcontextual study of a potential pit hearth at the Middle Paleolithic site of El Salt, Spain

Lucia Leierer [a,b,*], Ángel Carrancho Alonso [c], Leopoldo Pérez [d,e], Ángela Herrejón Lagunilla [f], Antonio V. Herrera-Herrera [a], Rory Connolly [a,b], Margarita Jambrina-Enríquez [a,g], Cristo M. Hernández Gómez [b,h], Bertila Galván [b], Carolina Mallol [a,b]

[a] Instituto Universitario de Bio-Orgánica Antonio González, Universidad de La Laguna, La Laguna, Santa Cruz de Tenerife, Spain
[b] Departamento de Geografía e Historia, Área de Prehistoria (Facultad de Humanidades), Universidad de La Laguna, Campus de Guajara, La Laguna, Santa Cruz de Tenerife, Spain
[c] Área de Prehistoria, Departamento de Historia, Geografía y Comunicación. Universidad de Burgos. Edificio I+D+I, Plaza Misael Bañuelos s/n, 09001, Burgos, Spain
[d] IPHES, Institut Català de Paleoecologia Humana i Evolució Social, Zona Educacional 4. Campus Sescelades URV (Edifici W3), 43007, Tarragona, Spain
[e] Àrea de Prehistoria, Universitat Rovira i Virgili (URV), Avinguda de Catalunya, 35, 43002, Tarragona, Spain
[f] Departamento de Física. Universidad de Burgos. Escuela Politécnica Superior (Campus Río Vena). Avda. Cantabria s/n, 090006, Burgos, Spain
[g] Departamento de Biología Animal, Edafología y Geología, Facultad de Ciencias, Sección de Biología, Universidad de La Laguna, La Laguna, Tenerife, Spain
[h] Departamento de Didácticas específicas. Facultad de Educación. Universidad de La Laguna, Tenerife, Spain

ARTICLE INFO

ABSTRACT

By studying combustion structures, which conceal information about anthropogenic activity, we might learn about their makers. This is especially important for remote time periods like the Middle Paleolithic, whose archaeological record comprises numerous combustion structures. The majority of these are simple, flat, open hearths, although a small number of features situated in pit-like depressions have been recorded. Given that hearths built on a flat surface can result in pit-like color alteration of the underlying sediment, accurate identification of pit hearths is a crucial step prior to behavioral interpretation. Here we present a comprehensive study of a possible pit hearth from the Middle Paleolithic site of El Salt, Spain, using a microcontextual approach combining micromorphology, lipid biomarker analysis, archaeomagnetism and zooarchaeology. This pit hearth involves a true depression containing a thick plant ash deposit. It reached very high temperatures, possibly multiple burning events and long combustion times. Morphologically distinct combustion structures in a single archaeological context may indicate different functions and thus a diverse fire technology, pointing to Neanderthal behavioral variability.

1. Introduction

Fire has played an important role in human lives since the late Pleistocene, as evidenced by different Middle Paleolithic and Middle Stone Age deeply stratified sites with archaeological fire throughout their sequence (e.g. Courty et al., 2012; Galván et al., 2014a; Goldberg et al., 2009b; Mallol et al., 2013a; Vaquero and Pastó, 2001; Wadley, 2006). Thus, we can study archaeological combustion structures from these remote periods to learn about their makers. These structures may convey information on aspects of pyrotechnology (e.g. fuel use, fire temperature, fire intensity, hearth maintenance) (Mentzer, 2012) which

as any other technology, reflects behavior and culture (e.g. Schiffer et al., 2001; Vitezović, 2013 and references therein). In order to obtain relevant information from an archaeological combustion structure, which is sedimentary in nature, it is necessary to apply geoarchaeological techniques (Miller, 2011). In recent years, different methodologies to study combustion structures as artifacts have been incorporated into archaeological method and theory (Mallol et al., 2017; Mallol and Henry, 2017; Mentzer, 2012, 2017; Miller, 2011) and there is a growing number of case studies on this topic (e.g. Aldeias et al., 2012; Haaland et al., 2017; Miller et al., 2013).

The Middle Paleolithic fire record comprises numerous combustion

---

features (Roebroeks and Villa, 2011 and references therein). The vast majority of these are generally described as simple open hearths, which are basic, flat structures without stone linings or surface preparation (James et al., 1989; Leierer et al., 2019a; Mallol et al., 2013a; Mallol et al., 2017; Meignen et al., 1989; Mellars, 1996; Olive and Taborin, 1989; Roebroeks and Villa, 2011). Research into this fire evidence from different perspectives has provided information about aspects of Neanderthal fire technology. For instance, although there is widespread evidence of wood ash and charcoal as the main fuel source, other fuel sources have been documented including bones (Costamagno et al., 2005, 2008; Théry-Parisot, 2002; Yravedra et al., 2016; Yravedra and Uzquiano, 2013), lignite (Théry-Parisot and Meignen, 2000) and liquid hydrocarbons (Courty et al., 2012). There is evidence of fire use to facilitate woodwork (Aranguren et al., 2018), for smoking purposes (Vidal-Matutano and Théry-Parisot, 2016) and the possibility to produce tar (Koller et al., 2001; Kozowyk et al., 2017; Niekus et al., 2019; Pawlik and Thissen, 2011; Schmidt et al., 2019; Wragg Sykes et al., 2015). Some of this evidence points towards pyrotechnological traditions involving fire use for purposes other than cooking and obtaining warmth and light. However, our knowledge on Neanderthal pyrotechnology is still very poor.

We might gain information from Middle Paleolithic combustion structures by focusing on their shape. A basic element of archaeological artifact analysis is morphology, a formal attribute that can be linked to culture and technology (Debénath and Dibble, 1994; Hunt and Bortolini, 2016). Although most Middle Paleolithic combustion structures are simple and flat, in a few cases they are delimited by stones or are concave, forming a depression or pit into the substrate. Middle Paleolithic fires placed in a depression have been reported at several sites (Table 1). These hearths have been variably described and analyzed (see Table 1). The function and other technological aspects of these pit hearths remain unknown.

Interpreting archaeological combustion structures in depressions as anthropogenic pit fires solely based on field observation can be misleading since experimental studies have shown that downward heat transfer in a fire made on a flat surface may result in a shallow, pit-like color alteration of the underlying sediment (Aldeias et al., 2016; Bellomo, 1993; Brodard et al., 2015; Mallol et al., 2013b; March et al., 2014; Pérez et al., 2017a). Such structures cannot be interpreted as anthropogenic pit hearths, as they did not involve intentional preparation of a pit or depression (Aldeias et al., 2016), raising the question of

Table 1
Sites with hearths placed in a depression, hearth description, and accompanying references.

Site	Hearth description	References
Champlost	15 cm deep accumulation of ashes, heated bones and lithics	(Farizy, 1994; Villeneuve and Farizy, 1989)
Abric Romaní	amongst numerous flat hearths, few built on natural depressions, few with a concave morphology	(Gabucio et al., 2017; Vallverdú Poch et al., 2012; Vaquero et al., 2001)
Oscurusciuto	2 m wide 15 cm deep hearth, containing heated bone, lithics, and rubified sediment	(Boscato and Ronchitelli, 2008; Villa et al., 2009)
Divje babe 1	one hearth with a 1 m diameter located in a depression	Paunovic et al. (2002)
Roca dels Bous	large hearth made in a 20 cm deep depression, at least used twice	Martínez-Moreno et al. (2004)
Kebara Cave	a few hearths with diameters over 80 cm and a thickness of around 25–45 cm, filled with ashes and charcoal, and hypothetically representing successive burning events	Meignen et al. (2007)
Hayonim Cave	large, well-delimited thick wood ash deposits with over 110 cm in diameter and a thickness of 10–12 cm	Goldberg and Bar-Yosef (2002)

how many correctly identified Neanderthal pit fires there are. Likewise, hearth cleaning activities might result in pit like structures showing ripped-up soil aggregates of the underlying substrate (Mallol et al., 2007).

Anthropogenic pit fires or pit hearths have been defined as combustion structures with a bowl- or U-shape, a depth of not more than 1 m and a diameter of 0.6–1 m (Groenendijk, 1987; Huisman et al., 2019; Peeters and Niekus, 2017). In archaeological context, the most commonly occurring pit hearths can be found in the Mesolithic record of the Netherlands, Belgium and northern Germany (Groenendijk, 1987), but also in other periods like the Bronze Age (Løvschal and Fontijn, 2019) and the Ninevite 5 period (Smogorzewska, 2012). There are a few ethnographic or ethnoarchaeological descriptions of pit hearths from native Americans (Skibo and Schiffer, 2008), seminomadic pastoralists (Zerboni et al., 2013) and contemporary hunter-gatherers (Mallol et al., 2007). A pit hearth is constructed through the excavation of the substrate, which limits the amount of oxygen in the fire (Mallol et al., 2017; Skibo and Schiffer, 2008). The temperatures reached in pit hearths seem to be lower than in flat hearths but more stable and spatially homogeneous (March, 1992; March et al., 2014; Peeters and Niekus, 2017). Thus, their morphology and thermal properties allow for different and more specialized functions than simple flat hearths. In the ethnographic record, there are pit hearths for hide smoking (Skibo and Schiffer, 2008), charcoal burning (Zerboni et al., 2013), and cooking (Mallol et al., 2007; Wandsnider, 1997). A study summarizing ethnographic data from cooking pits associates them with roasting big amounts of either plants or fatty meat "for extended periods of time and subjected to moderate to high heat" (Wandsnider, 1997, p. 28).

Given that the presence of pit hearths in the Middle Paleolithic would suggest technological or functional variation in fire use, microcontextual investigations of possible pit hearths can be of considerable value to behavioral research on Neanderthals (Aldeias et al., 2016; Haaland et al., 2017; Meignen et al., 2007). So far, successful identifications of Middle Paleolithic pit hearths using a microcontextual approach have been conducted in Kebara and Hayonim Cave (Goldberg and Bar-Yosef, 2002; Meignen et al., 2007).

At the Middle Paleolithic site of El Salt, a plausible pit hearth was found at the boundary of two depositional layers (stratigraphic units Xb and XI). This is so far, the only combustion feature that is not flat in the entire archaeological fire record of the site (a total of 83 combustion features). Normally at El Salt, combustion structures are simple, flat, with black sedimentary layers (here onwards BL) interpreted as charred topsoils (Leierer et al., 2019a; Mallol et al., 2013a). In contrast, the possible pit hearth does not exhibit a BL. Instead, it comprises a thick, whitish-grey sedimentary layer (WL) filling a small, irregular depression and reddish sediment (red layer or RL) at the base (Fig. 1, Fig. 2). In order to investigate the nature of this peculiar combustion feature, and to contribute to the understanding of Neanderthal fire technology, in this paper we applied a microcontextual and multidisciplinary approach combining micromorphology, lipid biomarker analysis, archaeomagnetism, and zooarchaeology.

2. Material and methods

2.1. Site

2.1.1. Setting

The Middle Paleolithic open-air site of El Salt (38°41′14″N, 0°30′32″W, 680 m a.s.l.) is located in Alcoy (Alicante, Spain). It rests against a 38 m high Paleocene limestone wall covered in tufa and travertine (Galván et al., 2014a; Galván et al., 2014b). The site has been dated by thermoluminescence between 60.7 ± 8.9 and 45.2 ± 3.4 Ka and comprises a 6.3 m thick stratified deposit divided into 13 lithostratigraphic units (Galván et al., 2014b; Garralda et al., 2014). The Middle Paleolithic sequence includes stratigraphic units from the lower of V to XII and can generally be described as horizontally bedded
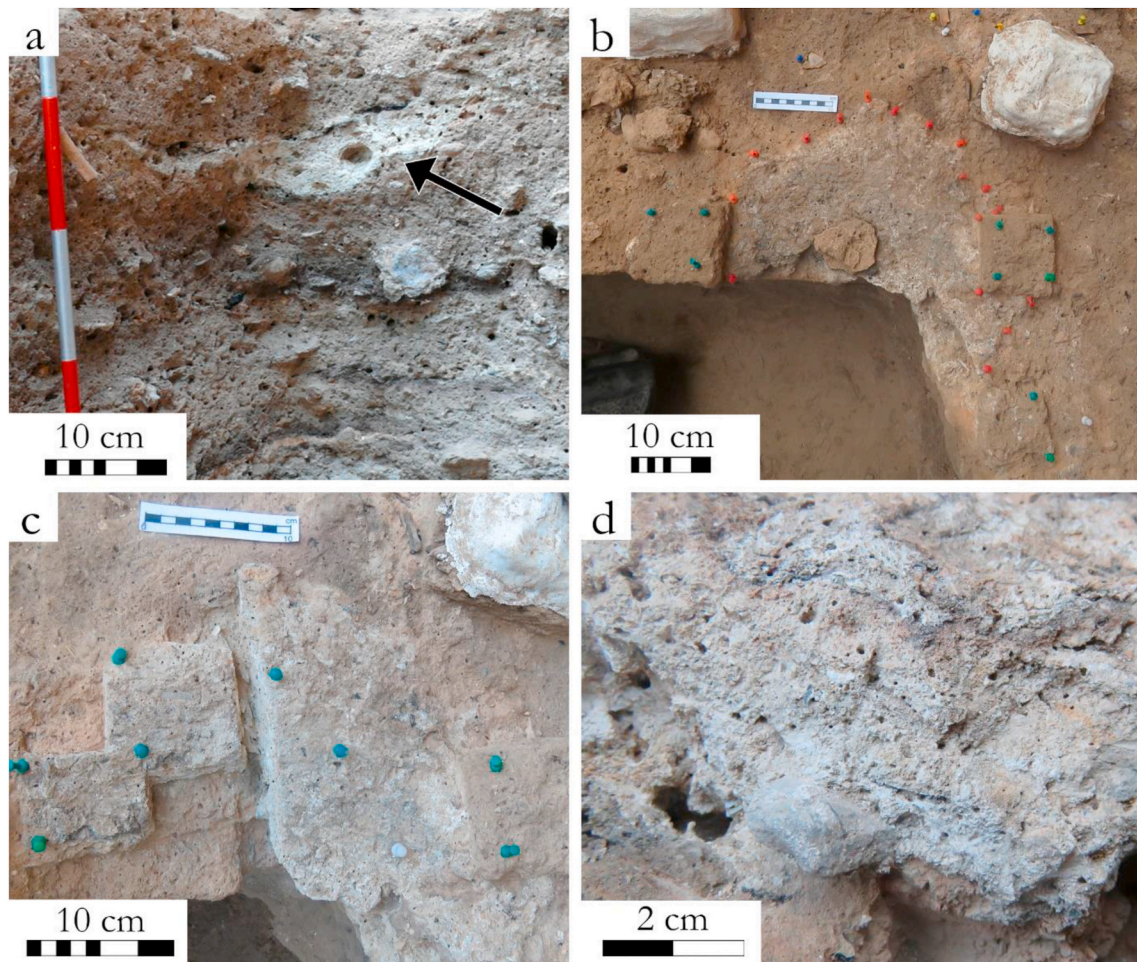
Fig. 1. Selected field photos of H77. a) Profile view of H77 from the year 2012. Note thick ash layer (arrow) that exhibits a slight bowl shape. b) Photograph of perimeter of the WL of H77 (red pins) and surroundings of hearth exposing the stratigraphic unit Lsg11 c) H77 during excavation while separated in two parts, in the left part, the WL has already been excavated and the RL and two archaeomagnetism samples are exposed. On the right part the upper surface of WL is exposed and has not been excavated there yet d) detailed view of the profile of the WL that was created by cutting the feature in two parts. The profile is viewed from the left part of the feature looking towards the right part. (For interpretation of the references to color in this figure legend, the reader is referred to the Web version of this article.)
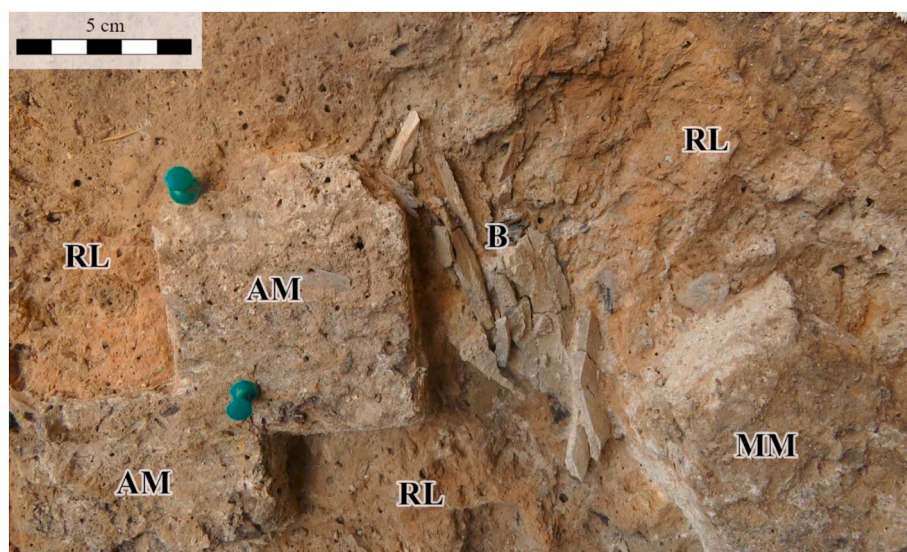
Fig. 2. Field photo of an area of H77 including the two archaeomagnetism samples of the WL (AM), the micromorphology block Salt-18-8 (MM), the underlying red layer (RL) and a deer tibia in 14 fire-cracked pieces (B). (For interpretation of the references to color in this figure legend, the reader is referred to the Web version of this article.)

geogenic sands containing archaeological remains and combustion residues, while these get more abundant from layer IX onwards (Fumanal García, 1994; Galván et al., 2014b; Leierer et al., 2019a).

Excavation and research from the University of La Laguna at this site are ongoing since 1986. Research involves multidisciplinary approaches at site formation and archaeological palimpsest dissection (Fagoaga et al., 2017, 2019, 2017; Galván et al., 2014a; Galván et al., 2014b; Machado et al., 2016; Machado and Pérez, 2015; Machado Gutiérrez et al., 2011; Mayor et al., 2020; Pérez et al., 2017b, 2020; Rodriguez Rodriguez et al., 2002; Rodríguez-Cintas and Cabanes, 2015; Sistiaga et al., 2014; Sistiaga Gutiérrez et al., 2011; Vidal-Matutano, 2016; Vidal-Matutano et al., 2017, 2018) as well as microstratigraphic analyses of hearths (Leierer et al., 2019a; Mallol et al., 2013b; Mallol et al., 2013a).

2.1.2. H77

Combustion structure H77, which was cut and partially lost during the excavations of 1960–61, was exposed during the 2018 field season. A clear pit shape was visible on the profile left by the 1960 excavations (Fig. 1a). It is located at the boundary between stratigraphic unit Xb and XI. Unit Xb is 10–14 cm thick and consists of archaeologically rich, slightly darker brown, sandy-silt (Fumanal García, 1994; Galván et al., 2014b; Leierer et al., 2019a). Unit XI has a variable thickness of 15–30 cm and shows black and white laminations underlain by a dark brown clayey-silty substrate (Fumanal García, 1994). The contact between Xb and XI is slightly undulating but very sharp.

The feature was covered by a lens of grey sandy silt (Field name: Lsg11), which was reported to be texturally different from the prevailing sedimentary facies in this unit. Directly beneath facies Lsg11 was the WL of feature H77. As can be seen on the 1960 profile (Fig. 1a). The WL was thicker towards the center of the feature, with a maximum thickness of 5 cm. Upon excavation of the WL, which was loose and massive and contained a few fresh rootlets, a sloping, reddish-brown (RL) sedimentary surface was exposed (see Figs. 1c and 2). The RL showed a massive appearance and was approximately 2 cm thick at the center of the feature, thinning out towards the periphery.

The archaeological assemblage stratigraphically associated with feature H77 comprises a concentration of calcined bone (n = 7), including a shaft fragment of around 8 cm. There were also a few cm long charcoal fragments and a few flint objects (n = 4). All the remains were found towards the bottom of the WL. The underlying RL deposit contained a larger archaeological assemblage, with 18 flint objects and 7 bone fragments.

2.2. Methods

2.2.1. Micromorphology

Archaeological soil micromorphology can aid in establishing stratigraphic relationships, identify sedimentary and archaeological components in their context, and can help with clarifying depositional and post-depositional processes (Courty et al., 1989; Goldberg and Macphail, 2009). In the case of a plausible pit fire, micromorphology can aid in distinguishing between a bowl shape created through heat penetration from a flat surface and an excavated pit.

Undisturbed blocks of sediment were extracted from within the feature (n = 3) and from outside in close proximity (n = 1) (see Fig. 2). The samples were processed at the Archaeological Micromorphology and Biomarker Research Lab (AMBI Lab), Universidad de La Laguna, Tenerife, Spain with the protocol published in Leierer et al. (2019a) and Leierer et al. (2019b).

The thin sections were observed under PPL (plane polarized light) and XPL (cross polarized light) using a Nikon Eclipse E200 polarizing microscope, with magnifications ranging between 20 and 100, and described following the guidelines of Stoops (2003) and Nicosia and Stoops (2017). The concept of microfacies approach was applied (Courty, 2001) to facilitate the understanding of micromorphological features and interpretations.

2.2.2. Lipid biomarker analysis – n-alkanes

In the last two decades, lipid biomarkers have gained importance in geoarchaeological research (Buonasera et al., 2019; Connolly et al., 2019; Herrera-Herrera and Mallol, 2018; Jambrina-Enríquez et al., 2018, 2019; Leierer et al., 2019a; Peters et al., 2005). Here, n-alkanes were extracted and measured to identify possible plant residues. A detailed protocol for obtaining these n-alkanes can be found in the supplemental material (Suppl. 1).

2.2.3. Total carbon, total inorganic, and total organic carbon analysis

A description can be found in the supplemental material (Suppl. 1).

2.2.4. Controlled heating experiments

In order to explore the rubification process of the RL in a sedimentary substrate such as that of El Salt, we conducted a series of controlled lab burns using presumably unburnt sediment from the stratigraphic unit XI. For each burn, approximately 0.8 g of sediment was placed into a ceramic crucible and heated in a muffle furnace (Nabertherm B180) to between 100 °C and 800 °C at intervals of 100 °C in oxidizing conditions. The furnace heating rate was ±26 °C/min (Kuo et al., 2008) and the designated temperature was kept constant for 1 h. After heating, the crucibles were extracted and cooled down. Color change and exact colors of the sediment were measured using the Munsell Soil Color Chart (Munsell Color (Firm), 2010).

2.2.5. Archaeomagnetic and rock-magnetic analyses

Four hand-blocks (samples) were collected from the H77 hearth. Two of the samples correspond to the WL (from 0.5 to 5 cm of thickness) (Fig. 2) and the other two to the subjacent RL (ca. 1–2 cm of thickness) (Fig. 1). Additionally, bulk (unoriented) sample from each facies was collected to carry out rock-magnetic analyses. A detailed description of sample extraction and analysis can be found in the supplemental material (Suppl. 1).

2.3. Faunal analysis

Zooarchaeological and taphonomic analyses were carried out following the standard methods (Lyman, 1994; Reitz and Wing, 2008). The protocol for these analyses can be found in the supplemental material (Suppl. 1).

3. Results

3.1. Micromorphology

Together, all the thin sections analyzed (6 from inside the feature, 2 from outside but closely related) provided a microscopic overview of the entire combustion structure. We identified 4 microfacies types (here onwards: MFTs) which can be correlated with the macroscopic field facies. These MFTs are, from base to top: MFT XI, MFT RL, MFT WL, and MFT Lsg11 (Fig. 3). Since lithology, components, and post-depositional processes share comparable characteristics throughout the sample set, they will be presented separately in the following paragraphs. Changes in frequency or composition within an MFT will be noted in the description of the MFTs. A detailed description of every microfacies unit can be found in the supplemental material (Suppl. 2).

3.1.1. Lithology

The lithological composition of the sample set is homogenous and characteristic of El Salt unit Xb, as has been previously documented (Leierer et al., 2019a). The sediment is sandy and detritic, with subrounded, quartz-rich limestone fragments, subrounded travertine and tufa fragments, and few subrounded quartz grains. These components show variations in abundance, degrees of weathering, and burning
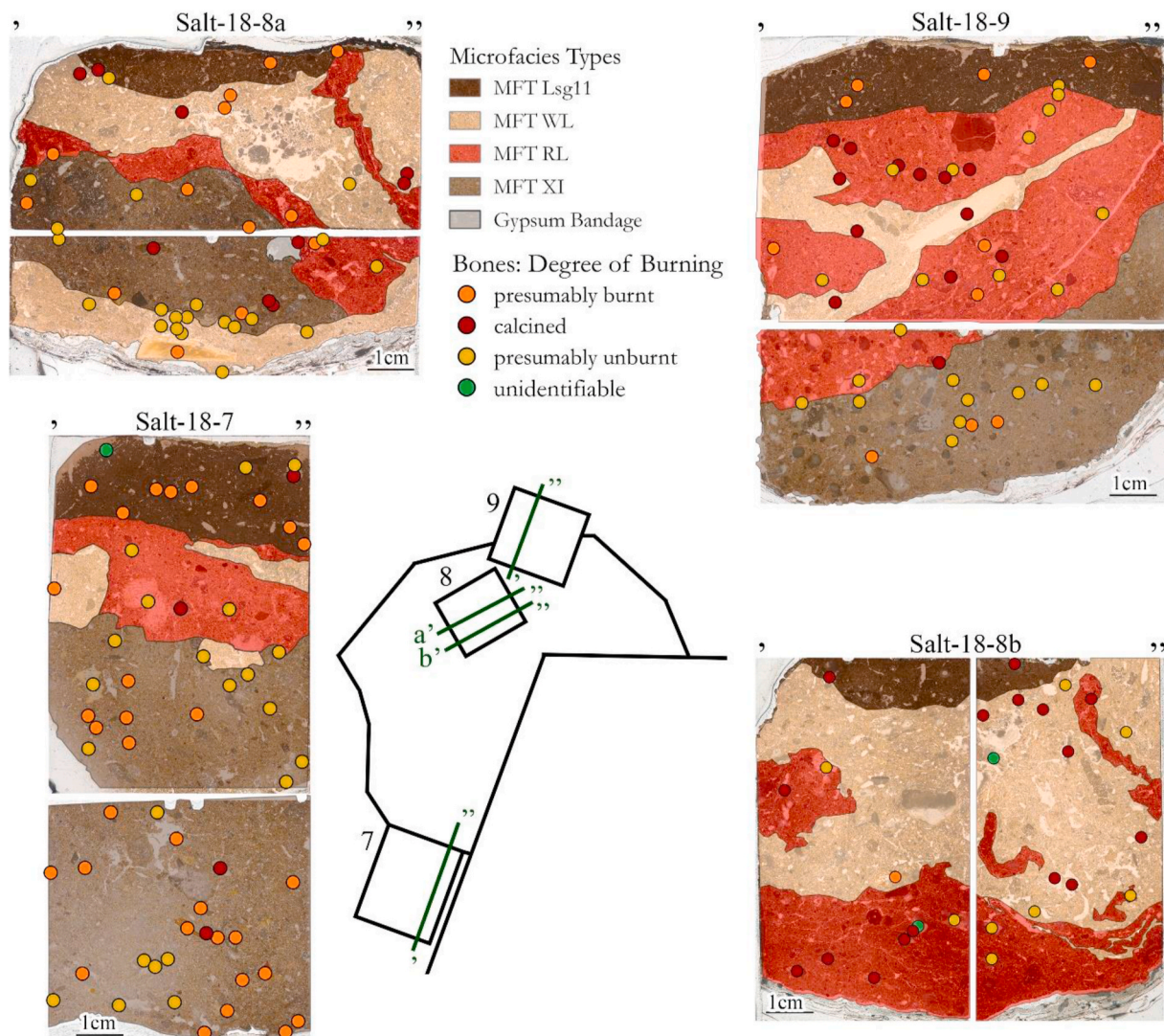
Fig. 3. Location of micromorphology block and their corresponding thin sections. Different colors indicate the microfacies types (MFT) and dots indicate the location and degree of burning of bones bigger than 1.5 mm. (For interpretation of the references to color in this figure legend, the reader is referred to the Web version of this article.)

throughout the different MFTs (see Suppl. 2). Some of the tufa fragments are brownish grey in PPL due to burning (Mallol et al., 2013a).

3.1.2. Other components

Anthropogenic and biogenic components are frequent in the sample set and are listed and described in Table 2 and presented in Fig. 4.

Microscopic faunal remains exhibit different degrees of burning. All bone fragments (excluding teeth) larger than 1.5 mm were mapped and their approximate degree of burning was subjectively classified, resulting in 173 bones with 4 possible degrees of burning: Calcined (n = 42), presumably burnt (n = 55), presumably unburnt (n = 73) and unidentified (n = 3) (see Fig. 3). The subjective classification was done according to optical differences in color (in PPL) and birefringence (in XPL), following reference material of experimentally heated bone and micromorphological guidelines for their characterization (Villagran et al., 2017). The distribution of the altered bones is random in all MFTs, while MFT XI and MFT Lsg11 have a predominance of heated bone and MFT RL and MFT WL a predominance of calcined bone. The abundance of bone is lower in the MFT WL compared to all other MFTs.

3.1.3. Post-depositional processes

The entire sample set is slightly disturbed by bioturbation. However,

the degree of bioturbation is small enough to enable a good comparison amongst the different MFTs. A majority of the void structure is dominated by channels and chambers. A small number of passage features could be observed as well. Nevertheless, physical transformation due to bioturbation is at a small scale, without disturbance of the general sedimentary structure. In a few instances, bioturbation took place at the boundary of two distinct MFTs, where sediment from one layer was mixed into the other layer in the form of a passage feature.

Part of the sample set shows post-depositional decalcification (Karkanas and Goldberg, 2010). MFT XI and MFT RL are more strongly decalcified than MFT Lsg11, whereas the ashes of MFT WL are the least decalcified. MFT XI and MFT Lsg11 contain massive coprolites and some voids are internally hypocoated with a phosphatic stain.

3.1.4. Microfacies types (MFTs)

3.1.4.1. MFT XI.
MFT XI has a dark brown color in PPL. At high magnification, the groundmass is brownish yellow, and it is evident that the dark brown color observed in the naked eye and at low magnification is due to the common presence of charcoal and black organic residues. In XPL, the b-fabric is only weakly crystallitic, indicating decalcification. The mineral grains are also affected by decalcification.

Table 2
Anthropogenic and biogenic components found in the sample set, their description, and their presence (marked with an "x") or absence (empty cell) in the specific MFT. Cells marked with an "(x)" represent a single occurrence of that component within the MFT.

Component	Description	MFT XI	MFT RL	MFT WL	MFT Lsg11
Ash	Woody and nonwoody plant-ash in different states of preservation			x	
Wood charcoal	Some fragments identified as pine	x		(x)	x
Black organic residues	Fine to medium sand size, possibly charred	x			x
Fibrous coprolite	Herbivore origin	x	x		x
Massive coprolite	Omnivore/carnivore origin	x	x		x
Celtis australis seed coats	Abundant throughout the sample set, some burned	x	x	x	x
Possible animal fat-derived char fragments	Very few particles of massive black matrix with vesicular voids and fissures commonly identified as charred liquid drops of fat (Clark and Ligouis, 2010; Goldberg et al., 2009b; Miller et al., 2009)	x			
Bones	Abundant throughout sample set, Predominantly microfauna and lower proportion of nondistinctive fragments, possibly macrofauna	x	x	x	x
Teeth	From rodents	x	x	x	
Flint flakes	Sand-sized flakes and flake fragments, some burned, visible as crazing (fine pattern of cracks) (Angelucci, 2017)		x		x

Intergrain microstructures are predominant and are complemented by subangular blocky microstructures. Voids are complex packing voids, channels, and chambers. Anthropogenic components like possible fat-derived char, charcoal, and bone are very abundant.

3.1.4.2. MFT RL. MFT RL exhibits massive reddish-brown sediment in PPL, devoid of organic material. The b-fabric resembles that of MFT XI. Depending on the position of the thin section within the feature, the RL is thicker, more reddish, without organic material (towards the center) or thinner, less red with very little organic matter (towards the periphery). In some areas, especially towards the center of the combustion structure, the upper part of the RL exhibits horizontal planes. Microstructure and voids are, apart from the planes, similar to that of MFT XI.

3.1.4.3. MFT WL. The thickness of the WL in thin section is up to 5 cm and the boundaries to over- and underlying units are sharp. MFT WL appears pale-yellowish brown in PPL and locally blueish grey or light grey in XPL. It is locally fibrous and composed exclusively of wood ash and unidentified plant ash. The light grey zones show a crystallitic b-fabric in XPL and contain calcium carbonate pseudomorphs of calcium oxalate, specifically calcitic wood ash rhombs (Fig. 5a–c), while the blueish grey zones lack rhombs and show scattered micritic crystals (Fig. 5d–i). The ashes in these areas are submicroscopic, which influences their interference color (Canti, 2003). Additionally, ash particles resembling plant structures are encountered within the blueish grey zones (Fig. 5i and j). They have a dark red color and are fibrous. Bigger particles have a cell structure preserved.

The microstructure is predominantly intergrain microaggregate and

vughy with occasional channels. MFT WL contains very few components – besides ash – the most abundant being bone fragments, followed by lower amounts of tooth fragments and *Celtis australis* seed coats.

3.1.4.4. MFT Lsg11. In regard to color, microstructure, voids, and the presence of anthropogenic components, MFT Lsg11 and MFT XI appear similar, however, MFT Lsg11 shows less decalcification of the matrix. The dark brown color of MFT Lsg11 is due to the presence of charcoal and black organic residues.

3.2. Lipid biomarkers – n-alkanes

We obtained *n*-alkane data from 8 loose sediment samples from inside the combustion feature (WL: n = 4, RL: n = 1) and from surrounding sediment on top (Lsg11: n = 1) and on the bottom (SU XI: n = 2) (Fig. 6). The concentration of total *n*-alkanes is rather low with an average of 0.113 µg per gram of dry sediment (µg/gds) with the highest concentration of 0.59 µg/gds (BM18 – Lsg11) and the lowest concentration of 0.005 in WL samples (BM37, BM43). We can broadly distinguish between samples from within the feature and samples around it. The RL and WL samples from within the feature are low in total alkane concentration (0.018 µg/gds n = 5) with dominant peaks in shorter chains between C18 and C21. The surrounding samples have a higher total alkane concentration of 0.656 µg/gds (n = 4) with dominant peaks in C31 and C35 and an odd-over-even predominance.

3.3. TC, TIC, and TOC

The results of TC, TIC, and TOC measurements can be found in the supplemental material along with a table depicting individual values.

3.4. Controlled heating experiments

Colors ranged from dark reddish-brown (on the Munsell soil color chart 5 YR 3/4) (100 °C) to reddish-yellow (5 YR 6/6) (800 °C) (see Fig. 7) (Munsell Color (Firm), 2010). We did not observe color change between 100 and 300 °C. At 400 °C, the sediment turned lighter in color but remained reddish-brown (5 YR 4/4). From 500 to 600 °C a change in color towards a very light reddish-brown was noted (5 YR 5/4), and towards light reddish-yellow at 700 and 800 °C (5 YR 6/6).

3.5. Archaeomagnetic results

Initial natural remanent magnetization (NRM) intensities of the WL are between 2.8×10^{-4} and 1.75×10^{-4} Am^2kg^{-1} while susceptibility varies between 5.5×10^{-6} and 4.0×10^{-6} m^3kg^{-1}. In the RL, NRM values vary between 4.5×10^{-4} and 4.3×10^{-5} Am^2kg^{-1} and susceptibilities oscillate between 5.45×10^{-6} and 9.6×10^{-7} m^3kg^{-1}. For both parameters, WL samples show higher values compared to the RL, suggesting that the concentration of ferromagnetic (*s.l.*) particles are higher in the WL.

Fig. 8 shows the values of the Königsberger (Q_n) ratio for both facies. The Q_n ratio (Koenigsberger, 1938; Stacey, 1967) is a magnetic parameter which relates to the remanent and induced magnetization ([$Q_n = NRM/(\chi H)$], where χ is the magnetic susceptibility and H the intensity of the local magnetic field). This parameter is commonly used to characterize burnt archaeological materials or igneous rocks and is considered a measurement of stability to indicate a sample's capability of maintaining a stable remanence such as thermal remanent magnetization (TRM). All values but one are over unity indicating that the magnetization is most probably of thermal origin and are in the range of other burnt archaeological and experimental materials such as hearths, pottery or fireplaces (e.g. Francés-Negro et al., 2019; Herrejón Lagunilla et al., 2019; Kapper et al., 2014).

The orthogonal NRM demagnetization diagrams obtained in both
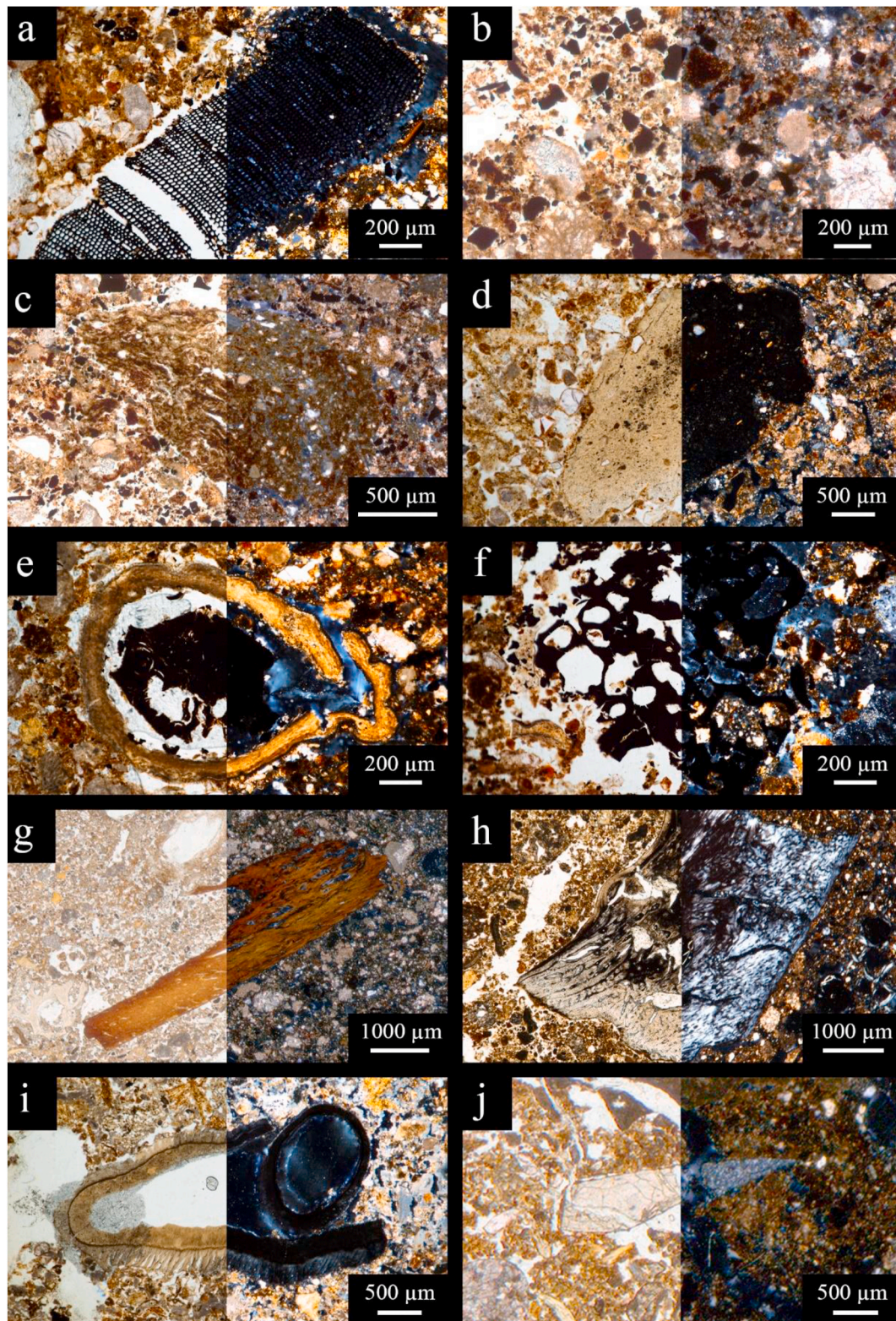
Fig. 4. Components mentioned in Table 2 as microphotograph. Each microphotograph represents PPL on the left side of the picture and XPL on the right side of the picture. a) charcoal, b) black organic particles, c) fibrous coprolite, d) massive coprolite, e) intact *Celtis australis* seed coat containing its charred seed, f) possibly fat derived char, g) heated bone, h) calcined bone, i) tooth, j) heated flint flake.

facies are characterized by high intensities of magnetization and stable and reproducible directions (Fig. 9). All specimens exhibit a low temperature secondary viscous component unblocking up to 200–250 °C. The characteristic remanent magnetization (ChRM) direction is isolated from 250 °C to 580–600 °C, systematically showing normal polarity.

Exceptionally, in a single case, the ChRM direction is defined between 200 and 500 °C in a RL sample (Fig. 9b). This behavior reflects a partial thermoremanent magnetization (pTRM) caused by the lower temperature reflected in this sample. A high-temperature (HT) component can be observed between 500 and 600 °C (Fig. 9b). The maximum
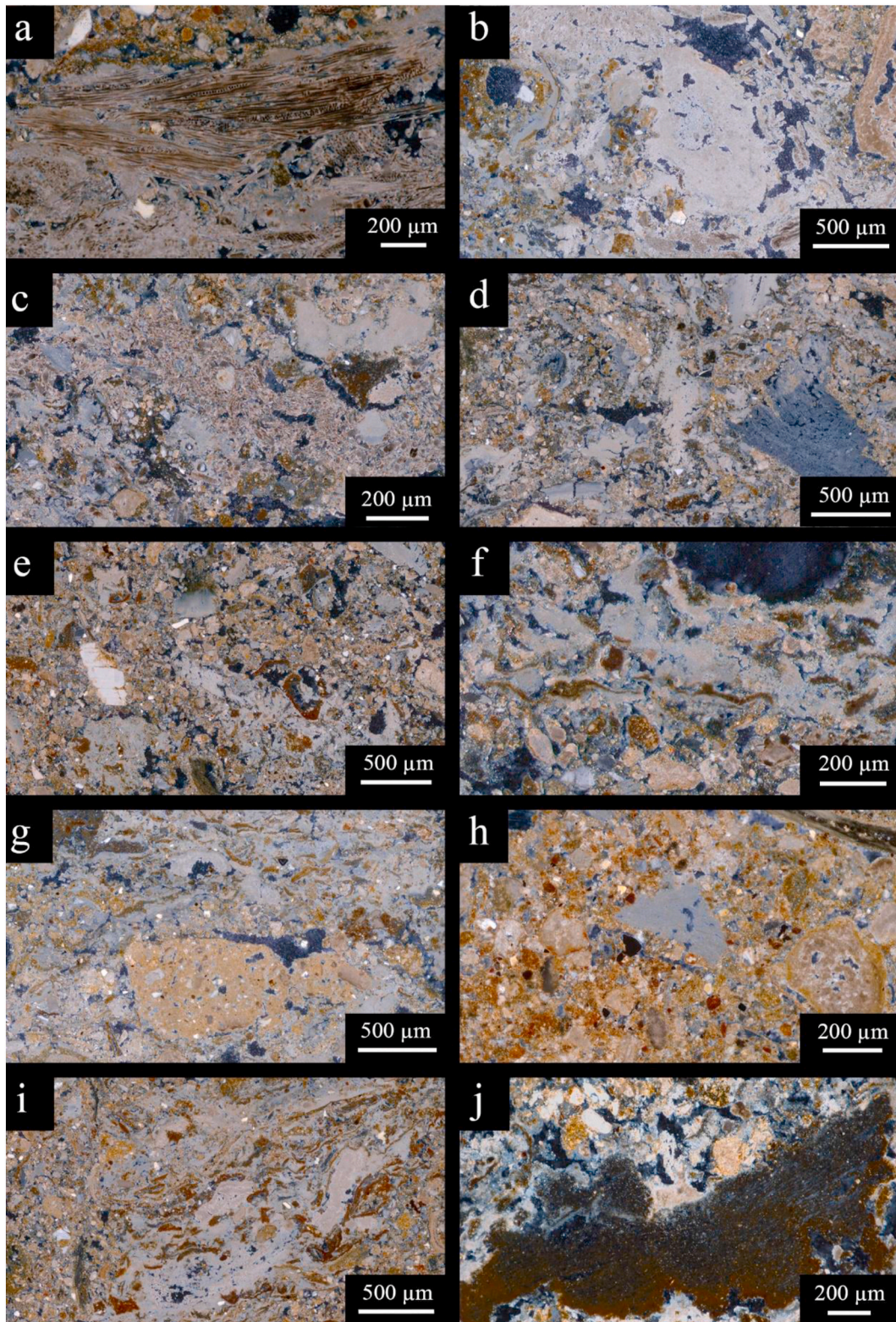
Fig. 5. Microphotographs of ashes taken in XPL: a) fresh wood ash in the form of calcium carbonate pseudomorphs of calcium oxalate (ash rhombs and rods), b) micritic mass of fine crystalline calcitic ash and carbonate pseudomorphs, c) fresh wood ash as carbonate pseudomorphs together with micritic mass of ashes, d) micritic mass of ashes of different crystal sizes according to the difference in color, e) micritic mass of ashes intermixed with sediment, f) micritic mass of ash crystals recrystallized around remains of reddish plant fiber, g) aggregate of RL sediment (passage feature) within micritic mass of ashes, h) aggregate of micritic ashes within the RL, i) accumulation of reddish plant fibers surrounded by recrystallized micritic ashes, j) close-up of large fibrous tissue fragment with preserved cell structure embedded in micritic ashes. (For interpretation of the references to color in this figure legend, the reader is referred to the Web version of this article.)
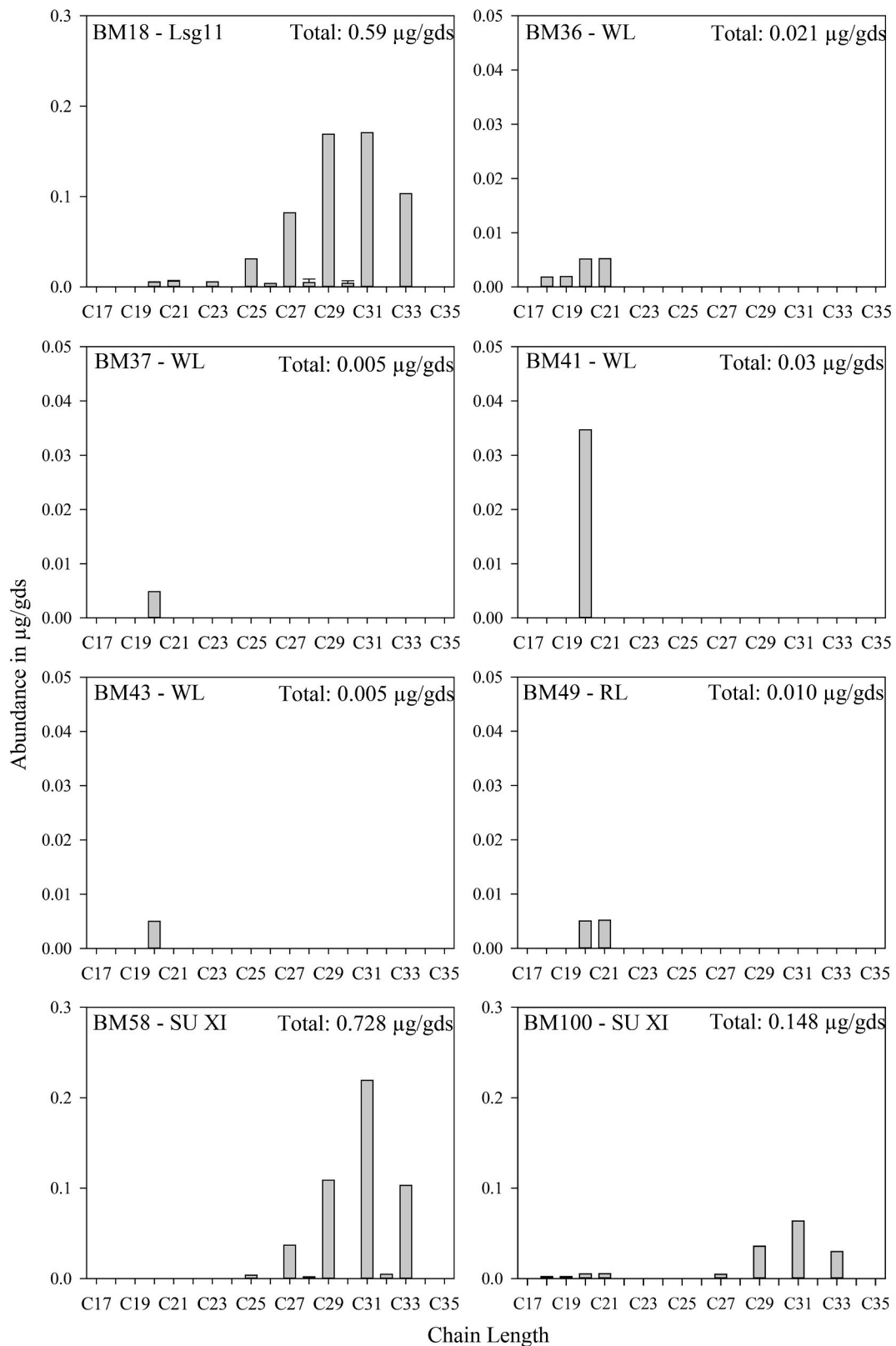
Fig. 6. N-alkane profiles of samples related to H77. Graphs show name of the sample, total alkane concentration and abundances of n-alkanes from chain length of C17 to C35 with two different scales on the y-axis. Error ranges are shown according to their standard deviation. Error ranges not visible are lower than 0.0009.

unblocking temperature (max T$_{UB}$) of the pTRM would indicate the maximum heating temperature experienced by this RL during its last heating. It seems logical to expect some variability in the temperatures reached by the burnt facies of prehistoric combustion features (e.g.

Carrancho et al., 2009), especially considering that the RL is underlying the WL, thus further away from the heat source. In any case, the dominant behavior in the NRM directional stability of both burnt facies is defined by highly magnetic, univectorial, stable normal polarity

Fig. 7. Color change after controlled burning of sediment from SU XI at different temperatures for 1 h. (For interpretation of the references to color in this figure legend, the reader is referred to the Web version of this article.)
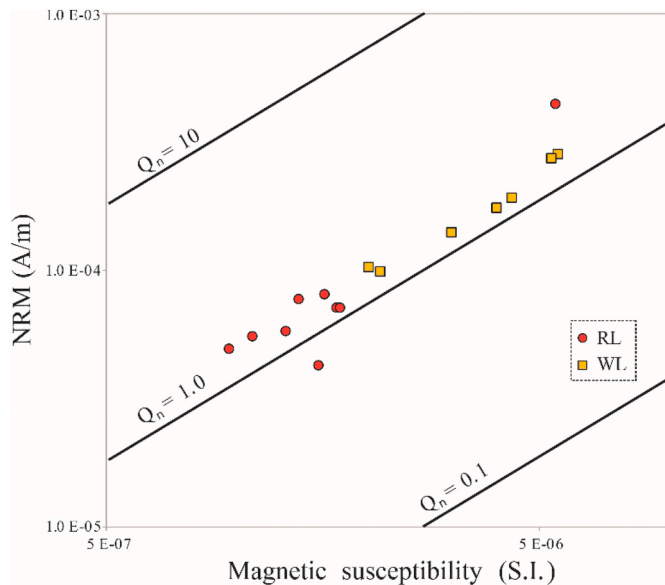
Fig. 8. The natural remanent magnetization (NRM) versus the bulk magnetic susceptibility (S.I.), showing lines of constant Koenigsberger ratio (Qn) between 0.1 and 10. RL = Red layer. WL = white layer. (For interpretation of the references to color in this figure legend, the reader is referred to the Web version of this article.)

diagrams most probably carrying a TRM. This observation is supported also by the Q_n ratio values and the thermomagnetic results explained below.

Regarding the magnetic properties, the WL maximum values of magnetization in the isothermal remanent magnetization (IRM) curves are higher than those from the RL. A similar trend is detected in thermomagnetic curves, in which a decreasing pattern in depth is also observed (Fig. 10a–j). The main magnetic carrier is in all cases a slightly substituted magnetite with Curie temperatures (T_C) around 580 °C. In general, there is a progressive decrease in the intensity of magnetization as a function of depth. Although the RL subsamples show some variability, their values are within the same order of magnitude (Fig. 10a–e). The decrease in the magnetization intensity as a function of depth is especially clear in the ash subsamples (Fig. 10f–j). In both facies, a total or very high degree of reversibility is observed, perhaps with the only exception of the deepest WL sample (Fig. 10i). In any case, the WL is magnetically more intense than the RL since it underwent higher temperatures generating a higher concentration of ferrimagnetic (*s.s.*) minerals (magnetite).

3.6. Faunal analysis

The bone remains associated with and recovered from H77 are very scarce, with only 13 NR (number of remains) that are split into 11 NME (minimal number of element) and 2 MNI (minimum number of individuals) (Table 3): one prime deer (*Cervus elaphus*) and one rabbit (*Oryctolagus cuniculus*). The remains are for the most part composed of long bone fragments, with a few instances of cranial or axial parts.

At a taphonomic level, all bone fragments exhibit thermal alteration, with a higher degree of surface modification in the layers closest to the heat source, as shown by the degree of burning and presence of cracks. For example, a single deer tibia was collected in 14 fire-cracked fragments (Fig. 2). However, signs of anthropogenic modification (e.g. slicing marks, scraping marks, dental imprints) are generally absent and only five fresh fractures were recorded (Table 4).

4. Discussion

Our multiproxy study indicates that the H77 combustion feature represents an in-situ pit hearth. Below, we discuss different lines of evidence from the geoarchaeological and zooarchaeological techniques applied, which provided clues about the nature of the feature, its degree of preservation, temperature estimates, and its possible use history.

4.1. H77: a well preserved in-situ pit hearth

Thick ash layers (of up to 20 cm) documented in Paleolithic contexts are typically interpreted as ash dumps based on their micromorphological features (Berna and Goldberg, 2008; Meignen et al., 2007). In the case of H77, an ash dump in the pit is improbable. First, the WL filling the small depression is composed of primary plant ash. Second, in agreement with experimental data from (Aldeias et al., 2016), the RL at the surface of the depression is thicker towards the center of the hearth (see Salt-18-9 in Fig. 3), indicating in-situ burning. The absence of a black layer underlying the H77 ash deposit is a notable difference from the other El Salt combustion structures, in which such black sedimentary layers are composed of charred decayed plant remains and excrements (Leierer et al., 2019a; Mallol et al., 2013a). Instead, H77 contains a thick RL completely devoid of organics. This RL resembles SU XI in all aspects (e.g. lithology, components, microstructure) except for the absence of organic matter and the red color, suggesting the same depositional source.

Further evidence of in-situ burning was obtained through archaeomagnetism. Our results clearly show that all the samples are highly magnetic and stable and that they have efficiently recorded the direction of the Earth's magnetic field at the time of the last burning and subsequent cooling. The magnetization intensity values are similar to those reported for burnt facies in prehistoric combustion structures (e.g. Carrancho et al., 2009; Kapper et al., 2014). The Qn ratio values point out that the mechanism of magnetization is most likely a thermoremanence (TRM). Furthermore, the stable orthogonal NRM demagnetization diagrams with reproducible directions and a good statistical grouping also indicate an efficient record of the magnetization through a TRM as well as a good preservation of the original combustion structure. If the samples had undergone severe mechanical reworking (e.g.: by trampling, bioturbation, etc.), the dispersion of the ChRM directions in the stereogram would be significantly higher with lower *k* values. Considering the reasonably low dispersion obtained (k = 111.3) and the age of this combustion structure (*ca.* 55 ky B.P.), the preservation level of H77 is very good.

This agrees with macro and microstratigraphic-scale observations. The contact between the RL and the WL is sharp, which is common in combustion structures (Mallol et al., 2017), and does not show any signs of post-depositional disturbance. No microscopic ripped-up clasts or
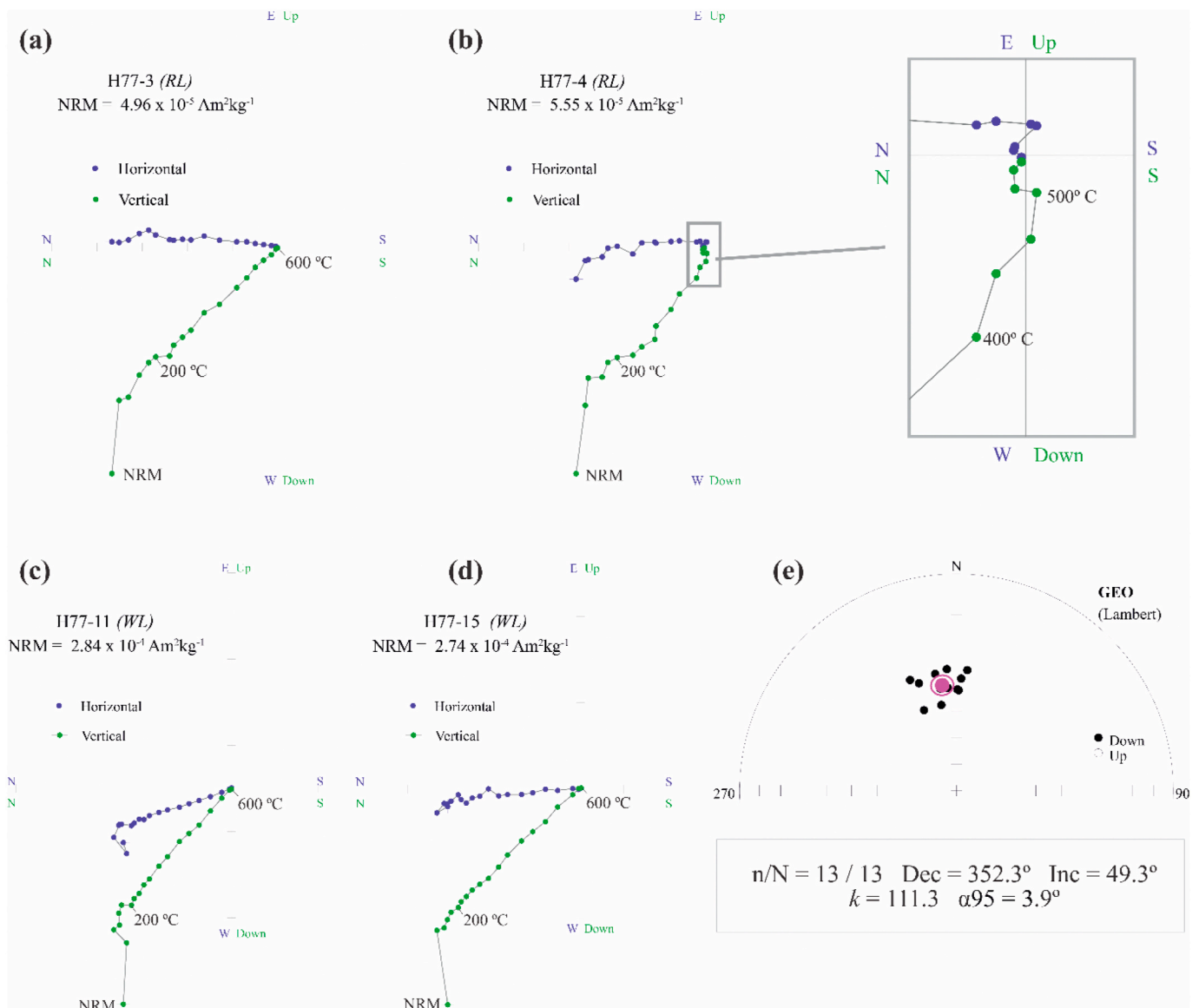
Fig. 9. (a–d) Representative orthogonal NRM thermal demagnetization plots from hearth H77. Green (blue) symbols represent the vertical (horizontal) projections of vector endpoints. The sample code, intensity (NRM) and type of facies studied are shown for each sample. RL = red layer; WL = while layer. For clarity, the last steps of panel b are blown up showing a high-temperature component. (e) An equal-area projection of all ChRM directions, with the mean direction calculated at sample level and the α95 confidence circle (in pink). n/N = number of specimens considered/analyzed; Dec. = declination; Inc. = inclination; k = precision parameter; α95, semi-angle of confidence. (For interpretation of the references to color in this figure legend, the reader is referred to the Web version of this article.)

mixing between the two layers was observed, except for two instances of ash embedded in the RL, which will be discussed in the fire use history section below. The absence of ripped-up aggregates from underlying substrate speaks against hearth cleaning activities and thus incidental production of a pit (Mallol et al., 2007). Regarding the formation of the pit, it could have been intentionally excavated or it could have been present prior to the fire as a natural depression.

4.2. Estimating burning temperatures

Reddening and absence of organics together point towards high-temperature combustion. Organic matter is oxidized between 500 and 550 °C, where it gets converted to carbon dioxide and ash (Heiri et al., 2001; Wang et al., 2011). At these temperatures, both fresh and charred organics disappear from the sedimentary matrix. Thus, the RL must have been exposed to such temperatures for some time. Rubification is the reddening of iron-containing soils or sediment from heat (Röpke and

Dietl, 2017). Experiments have shown that organic substrates rubify less than inorganic sediments (Aldeias et al., 2016; Berna et al., 2007; Canti and Linford, 2000; Mallol et al., 2013a; March et al., 2014). Nevertheless, the temperature at which reddening occurs is unclear. Different experimental burning studies report rubification at different temperatures which taken together yield a broad range (250 °C–800 °C) (Berna et al., 2007; Gualtieri and Venturelli, 1999; Mathieu and Stoops, 1972; Röpke and Dietl, 2017), suggesting that sediment type may be an influential variable. Some sediments show no reddening even at high temperatures (Berna et al., 2007; Canti and Linford, 2000). In an experimental study in which fires were made on the natural substrate surrounding the El Salt site, only 2 out of 25 of the resulting combustion structures yielded reddish layers at their base (Mallol et al., 2013b). One structure, with a 9 mm thick patchy RL directly underneath the ash layer was from a fire made on artificially wet sediment, fueled with a total of 24.4 kg of pine wood for 6–7 h (Mallol et al., 2013b). The resulting RL was interpreted to originate from mineral dehydroxylation upon fast
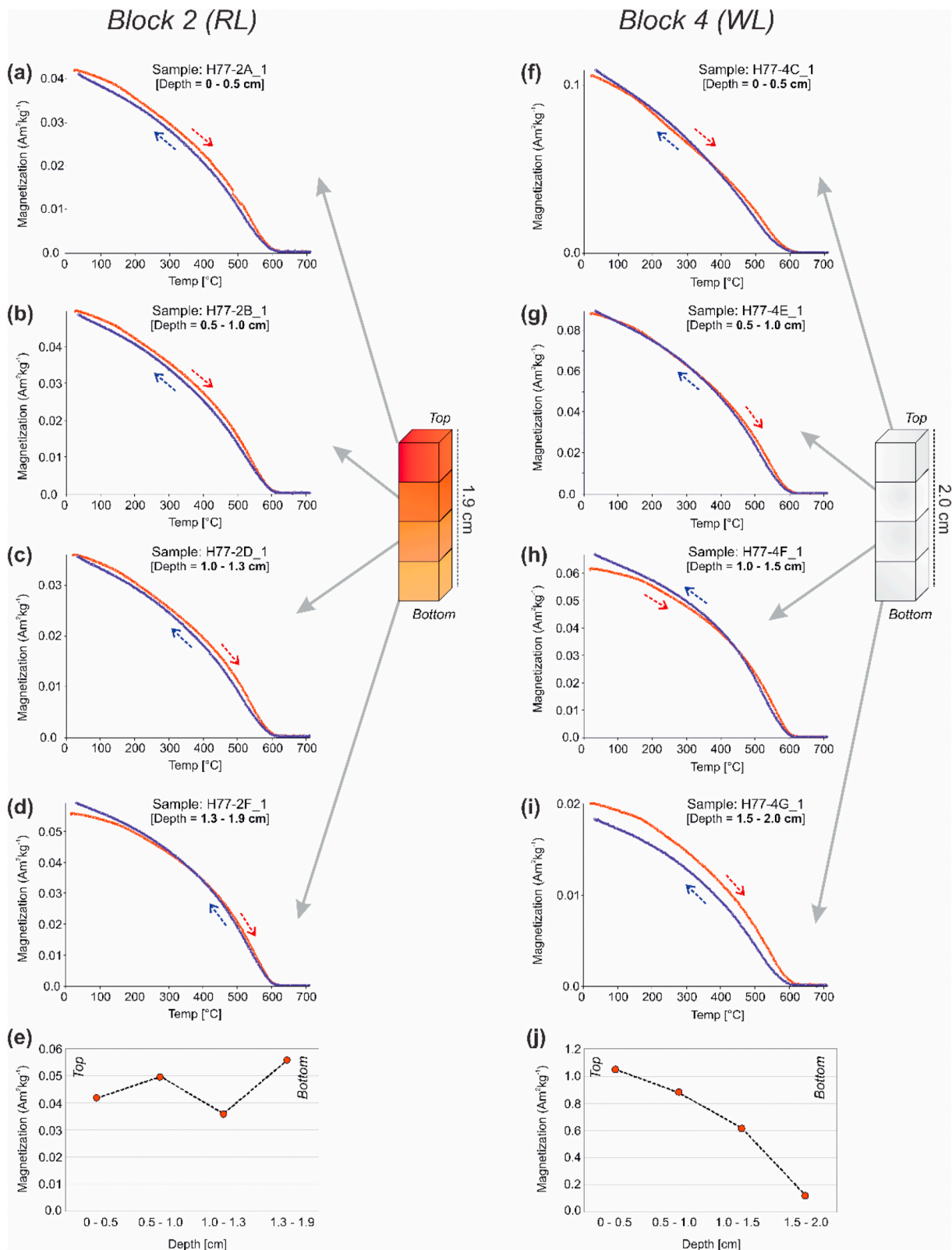
Fig. 10. Thermomagnetic curves analyzed as a function of depth for (a–e) block 2 (red-layer or RL) and (f–j) block 4 (white layer or WL). Sample code, depth and magnetization intensity are indicated for every sample. Heating (cooling) cycles are shown in red (blue) with their respective arrows. Panels e and j represent the variation of the magnetization intensity at room temperature for the heating cycle of every sample at different depths for both blocks. (For interpretation of the references to color in this figure legend, the reader is referred to the Web version of this article.)

Table 3
Measures of abundance and quantification of taphonomic alterations of faunal remains in H77.

Taxa	Abundance			Taphonomic alterations					
	NR	MNE	MNI	Thermal Alt.	Fracture fresh	Fracture dry	Mixed Fracture	Manganese	Root-marks
Cervus elaphus	3	3	1 (Prime)	3	1		2	2	
Oryctolagus cuniculus	1	1	1	1	1	4		1	
Medium size	3	1	–	3	2		1	1	1
Small size	1	–	–	1				1	
Undetermined	5	1	–	3	1			2	1
	13	6	2	11	5	4	3	7	2

Table 4
Main features observed in the H77 heated bone.

Taxa	Anat. Element	Facies	Fragment	Type	Origin	Agent	Distribution	Color	Modification
Cervus elaphus	Ribs	WL	550	Thermal alt.	Fire	Anthropic	Total	Grey	Cracks
Cervus elaphus	Radius	WL	500	Thermal alt.	Fire	Anthropic	Total	Black	Cracks
Cervus elaphus	Tibia	WL	050	Thermal alt.	Fire	Anthropic	Total	Bl/G/Wh	Cracks
Oryctolagus cuniculus	Long bone	RL	050	Thermal alt.	Fire	Anthropic	Total	Black/Grey	–
Medium size	Cranial	RL	050	Thermal alt.	Fire	Anthropic	Total	Grey/White	Scaling
Medium size	Long bone	RL	050	Thermal alt.	Fire	Anthropic	Partial	Brown/Grey	–
Medium size	Long bone	RL	050	Thermal alt.	Fire	Anthropic	Total	Black	–
Small size	Long bone	WL	050	Thermal alt.	Fire	Anthropic	Total	Brown/Black	–
Undetermined	Cranial	WL	051	Thermal alt.	Fire	Anthropic	Total	White	Cracks
Undetermined	Undetermined	RL	050	Thermal alt.	Fire	Anthropic	Total	Grey/White	Cracks
Undetermined	Long bone	RL	050	Thermal alt.	Fire	Anthropic	Total	Brown/Grey	–

water evaporation rather than high temperatures (Mallol et al., 2013a). The other structure yielded a 0.5 cm thick RL directly underneath the ash layer. It resulted from a fire made on very compact, inorganic sediment fueled for 3 h (Mallol et al., 2013a). Our results from experimental lab burning of unit XI sediment, which comprises abundant black organic residues and charcoal fragments (see MFT XI), showed that rubification started at 500 °C and was strongest at 700–800 °C (see Fig. 7).

From the experiments described above, we can reasonably speculate that the H77 combustion structure represents three possible scenarios: a pit hearth 1) made on organics-containing sediment whose temperatures (at the substrate) may have reached at least 500 °C, or 2) made on inorganic sediment whose temperatures might have not necessarily exceeded 500°, or 3) made on wet sediment. The presence of microscopic horizontal fissures observed at the upper part of the H77 RL in the samples closest to the center of the structure suggest that the substrate reached high temperatures, as reported in previous experiments (Mallol et al., 2013b; Mallol et al., 2013a). As discussed below, our lipid biomarker and archaeomagnetism data also agree with this hypothesis and are both against the wet substrate scenario and the inorganic sediment scenario.

Our *n*-alkane data indicate that the RL and WL were exposed to high heat. These sedimentary layers yielded low *n*-alkane concentrations with dominant peaks at C20 and C21 indicative of degradation. A record of degradation implies that the original sediment contained some organic matter. Possible causes for degradation are either thermal (Eckmeier and Wiesenberg, 2009) or microbial (Brittingham et al., 2017). Microbial degradation would generally affect the whole sample set, and the surrounding sedimentary facies (Lsg11 and SU XI) showed better preservation and no signs of alteration, hence microbial degradation is unlikely. Thermal degradation was shown in experimental work on *n*-alkanes of *Celtis australis* leaves, bark, branches, and twigs, which represent similar *n*-alkane patterns as the H77 assemblage with dominant peaks at C20 at temperatures higher than 350 °C (Jambrina-Enríquez et al., 2018). Another study on a combustion structure assemblage from El Salt SU X showed comparable patterns in several BL and WL (Leierer et al., 2019a). Comparing our data with these results, an estimated burning temperature of much higher than 350 °C can be proposed for the H77 fire. Comparing our data to Wiesenberg et al. (2009), who conducted charring experiments with rye and maize, temperatures might have even exceeded 500°.

Regarding our archaeomagnetism data, the high degree of thermomagnetic reversibility recorded in the thermomagnetic curves (coincidence between the heating and cooling cycles) indicates that both WL and RL underwent high heating temperatures, most likely > 600–700 °C. Otherwise, they would not show such high reversibility upon laboratory re-heating to those temperatures as probably, their ferromagnetic mineralogy would not be stabilized. The stable and reproducible directional behavior of the NRM orthogonal demagnetization plots is also compatible with high-temperature heating.

In a single case, a p-TRM seems to have been recorded in a RL sample that would have reached a maximum temperature of 460–500 °C (Fig. 9b). This might be explained by the internal temperature variability expected for simple anthropogenic combustion structures (Canti and Linford, 2000). The considerable thickness of the ashes of the H77 hearth (up to 5 cm) is also indicative that a significant amount of fuel was burnt, which would favor reaching high temperatures. In any case, the high NRM intensities observed, Q_n ratio values > 1, stable orthogonal NRM demagnetization plots with quite reproducible directions and a high reversibility in the thermomagnetic curves all indicate a high-temperature heating and the record of a TRM. These criteria have already been observed in other archaeomagnetic studies on prehistoric fires as proof of stable remanences and well-heated materials (e.g. Carrancho et al., 2012).

In the literature, burning temperatures of pit hearths are still being discussed. There is a consensus that pit fires do not reach the same high temperatures as flat hearths (March et al., 2014; Peeters and Niekus, 2017) due to the insulating effects of the pit depression and reduced oxygen input (Mallol et al., 2017), which also renders combustion slower, incomplete and more charcoal-rich (March, 1992; March et al., 2014). Another factor which limits burning temperatures is the rapid infilling of the pit with ash and charcoal, which are both thermally insulating (Aldeias et al., 2016; Canti and Linford, 2000; March et al., 2014). March et al. (2014) report average temperatures above ground in experimental hearths with simple flat hearth temperatures at 335 °C and pit hearth temperatures at 273 °C. Other experimental flat hearths reach maximum mean temperatures of 600 °C (Bellomo, 1993) or their maximum temperatures range from 600 to 1000 (Bentsen, 2012, 2013;

Braadbaart et al., 2012; Canti and Linford, 2000; Sievers and Wadley, 2008; Stiner et al., 1995). Evidently higher temperatures than reported in March et al. (2014) can be reached.

Factors that seem to influence temperatures reached on the surface are the number of heatings, the quantity of fuel, conductivity of the substrate as well as the position within the combustion structure (Carrancho and Villalaín, 2011) and in the subsurface are amongst others intensity of heat, duration, sedimentary moisture and compaction (Aldeias et al., 2016).

Despite these conditions and considering our different proxies, our temperature estimates for H77 would be between 500 °C and 600 °C for the RL. These temperatures are relatively high compared to other experimental values of pit hearths but might not be impossible to reach. Even if temperatures reached are slightly lower than in the experimental flat fires, if kept burning for long enough, temperatures between 500 and 600 °C might be reached in the uppermost few centimeters (Aldeias et al., 2016).

4.3. Approaching the use history of the H77 pit hearth: fuel and repeated use

Microscopically, the H77 plant ash observed throughout the WL samples consists of well-preserved calcium carbonate pseudomorphs of calcium oxalate in a mass of fine crystalline, birefringent, calcareous material (Canti, 2003), as has been previously described for partially dissolved and recrystallized wood ash (Canti, 2003; Shahack-Gross et al., 2008). Recrystallization of wood ash is a common diagenetic process in archaeological contexts (Goldberg et al., 2009b; Karkanas et al., 2007; Madella et al., 2002; Shahack-Gross et al., 2008; Zerboni, 2011). In H77, there is also residual reddish fibrous matter mixed with the recrystallized ash (see Fig. 5i and j), resembling experimentally burned moss (Mallol et al., 2017). However, the color of this fibrous matter does not suggest charring or calcination. Given that the alkane signature of the WL does not indicate input of fresh plant matter (see Fig. 6), a possible explanation might be plant pseudomorphs, which are common in ashes (Mallol et al., 2017 and references therein) associated with clay that may have been coating the plant at the time of combustion (Goldberg et al., 2009a). For now, the nature of the plant fuel that was mixed with wood in H77 remains unknown.

How intense was the use of the H77 pit hearth? Considering possible volume reduction of the original ash deposit due to slight dissolution and compaction (Schiegl et al., 1994, 1996), the preserved ash volume in H77 is considerable. This could have resulted from a single, long-duration combustion event or a complex use history involving different relighting episodes. Both scenarios may involve massive, thick ash deposits (Mallol et al., 2007). Weiner et al. (2002) state that the absence of charcoal in a hearth and therefore the white color of its ashes might be indicative of repeated burning at the same location. H77 RL and WL contained only one charcoal fragment in sample Salt-18-8a, with a diameter of about 1 cm, fractured in-situ, and concentrated in the upper third of the WL.

Slight reworking, relighting, or repeated use of the structure is evidenced in sample Salt-18-8b, which exhibits two ash lenses embedded in the RL, and sample Salt-18-7, which shows thin ash concentrations underlying the RL. Such evidence points to the structure's complex formation history. These ash lenses and concentrations have not been disturbed by bioturbation, so it is highly likely that they are in-situ. According to previous experiments, relighting a hearth after a short time might not always show characteristic stratigraphic features and thus go unnoticed (Mallol et al., 2013b), while relighting of hearths after a long hiatus can be recognized as stacked combustion structures that either have successions of BL and WL or laminated WLs (Berna and Goldberg, 2008; Goldberg, 2003; Goldberg et al., 2009b; Meignen et al., 2007). Here, it is unlikely that there was a long hiatus between the burning events since sedimentation would have affected the entire surface of the hearth and not only a small patch within the combustion

feature. It is more likely that part of the sediment from the wall of the pit fell on top of the initial ash layer and was possibly rubified upon subsequent burning.

Finally, additional information on the use history of the H77 pit hearth comes from the faunal assemblage contained in the ash deposit. Although it is too small to draw any conclusions about anthropogenic activity besides intentional burning, it seems clear that the bone remains represent animal refuse (mainly red deer) that was tossed in the flames. Unintentional burning of bone fragments that might have been lying on the surface is unlikely, as all the bone specimens are strongly heated to levels close to calcination, which has been experimentally shown to correspond to bone in direct contact with fire (Mallol et al., 2013a; Pérez et al., 2017a). The bone could have been tossed in the fire as fuel or for other purposes or reasons.

4.4. Final remarks

The H77 combustion structure is located at the interface of stratigraphic units X and XI. It is embedded in stratigraphic unit XI and covered by stratigraphic unit X, suggesting a possible correlation with human occupations taking place sometime between the end of the formation of the unit XI deposit and the deposition of unit X. Archaeological excavation of El Salt unit XI has only just begun and there is no fire record to compare or results with. If we compare H77 with the unit X fire record, which has been extensively studied (Leierer et al., 2019a; Mallol et al., 2013a; Vidal-Matutano, 2016; Vidal-Matutano et al., 2017, 2018), it is one of a kind. Neither the morphology nor the temperature reached in H77 has been encountered in El Salt before. The microscopic appearance of the ashes and the fibrous material is also undocumented. Future experiments to generate ash from different plants are needed to determine possible fuel sources.

The differences in morphology between flat hearths and pit hearths are considerable. In artifacts differences in morphology represent variability in function and hence culture and technology (Debénath and Dibble, 1994; Hunt and Bortolini, 2016). Given that combustion structures are artifacts, morphologically distinct combustion structures may indicate different functions and thus a diverse fire technology. Even though we do not know the function of H77, we can assume it is different by comparing it with ethnographic cases. Pit hearths are normally used for hide smoking (Skibo and Schiffer, 2008), charcoal burning (Zerboni et al., 2013), and cooking (Mallol et al., 2007; Wandsnider, 1997). While flat hearths might also be used for cooking, it is likely that the food gets affected differently by a variation in heat transfer (Mallol et al., 2017). Thus, the deliberate use of a pit fire reflects variation in fire technology. Regarding the comparably high temperatures reached in this fire, there might have been an intent to keep this fire burning with such high temperatures. This is evidence of Neanderthal behavioral variability (i.e. Burke, 2006; Kuhn, 1995; Scott, 2011; Speth, 2010).

5. Conclusion

H77 is an in-situ combustion structure that we interpret as an anthropogenic fire made in a pit by Neanderthal groups living at El Salt prior to the unit X occupations. Whether the pit was dug out or was a natural depression remains unknown. Our multiproxy data indicate that the fire reached high temperatures (500–600 °C in the RL) and possibly had a complex use history. The fuel consisted of a mix of wood and another undetermined plant and during its use, animal refuse (especially ribs, radius, and tibia of red deer) was tossed in it.

So far, H77 is the only pit hearth documented at the site, which has yielded 83 combustion features, and one of the few pit hearths documented in the Eurasian Neanderthal record. The addition of well-documented pit hearths to the Neanderthal record implies variability in fire technology and supports overall Neanderthal behavioral variability, an aspect that had not previously been explored through the fire record.

For this study, we have applied a novel multiproxy, microcontextual approach. Although soil micromorphology has been previously used to reconstruct anthropogenic fire formation processes, there are very few studies combining this technique with lipid biomarker analysis to pin down fuel sources and burning temperatures. Coupling these two techniques with archaeomagnetism is also unprecedented. In order to advance our knowledge on the function and technological variability of Neanderthal fire, more Middle Paleolithic combustion structures need to be studied using similar multiproxy, microcontextual approaches. For the specific case of H77, further experiments, including ones with single and multiple-use pit hearths made on organic, inorganic, and wet sediment, need to be performed to test our present hypotheses.

Declaration of interests

The authors declare that they have no known competing financial interests or personal relationships that could have appeared to influence the work reported in this paper.

Acknowledgments

Appendix A. Supplementary data

Supplementary data to this article can be found online at https://doi.org/10.1016/j.jas.2020.105237.

References

Aldeias, V., Dibble, H.L., Sandgathe, D., Goldberg, P., McPherron, S.J., 2016. How heat alters underlying deposits and implications for archaeological fire features: a controlled experiment. J. Archaeol. Sci. 67, 64–79.

Aldeias, V., Goldberg, P., Sandgathe, D., Berna, F., Dibble, H.L., McPherron, S.P., Turq, A., Rezek, Z., 2012. Evidence for neandertal use of fire at roc de Marsal (France). J. Archaeol. Sci. 39 (7), 2414–2423.

Angelucci, D.E., 2017. Lithic artefacts. In: Nicosia, C., Stoops, G. (Eds.), Archaeological Soil and Sediment Micromorphology. Wiley, pp. 223–230.

Aranguren, B., Revedin, A., Amico, N., Cavulli, F., Giachi, G., Grimaldi, S., Macchioni, N., Santaniello, F., 2018. Wooden tools and fire technology in the early Neanderthal site of Poggetti Vecchi (Italy). Proc. Natl. Acad. Sci. U. S. A 115 (9), 2054–2059.

Bellomo, R.V., 1993. A methodological approach for identifying archaeological evidence of fire resulting from human activities. J. Archaeol. Sci. 20 (5), 525–553.

Bentsen, S.E., 2012. Size matters: preliminary results from an experimental approach to interpret Middle Stone Age hearths. Quat. Int. 270, 95–102.

Bentsen, S.E., 2013. Controlling the heat: an experimental approach to middle stone age pyrotechnology. S. Afr. Archaeol. Bull. 68 (198), 137–145.

Berna, F., Behar, A., Shahack-Gross, R., Berg, J., Boaretto, E., Gilboa, A., Sharon, I., Shalev, S., Shilstein, S., Yahalom-Mack, N., Zorn, J.R., Weiner, S., 2007. Sediments exposed to high temperatures: reconstructing pyrotechnological processes in late Bronze and iron age strata at tel dor (Israel). J. Archaeol. Sci. 34 (3), 358–373.

Berna, F., Goldberg, P., 2008. Assessing Paleolithic pyrotechnology and associated hominin behavior in Israel. Isr. J. Earth Sci. 56 (2), 107–121.

Boscato, P., Ronchitelli, A., 2008. Strutture di combustione in depositi del Paleolitico medio del Sud Italia. Int. J. Anthropol. Suppl, 218–225.

Braadbaart, F., Poole, I., Huisman, H.D., van Os, B., 2012. Fuel, Fire and Heat: an experimental approach to highlight the potential of studying ash and char remains from archaeological contexts. J. Archaeol. Sci. 39 (4), 836–847.

Brittingham, A., Hren, M.T., Hartman, G., 2017. Microbial alteration of the hydrogen and carbon isotopic composition of n-alkanes in sediments. Org. Geochem. 107, 1–8.

Brodard, A., Lacanette-Puyo, D., Guibert, P., Lévêque, F., Burens, A., Carozza, L., 2015. A new process of reconstructing archaeological fires from their impact on sediment: a coupled experimental and numerical approach based on the case study of hearths from the cave of Les Fraux (Dordogne, France). Archaeol Anthropol Sci 8 (4), 673–687.

Buonasera, T., Herrera-Herrera, A.V., Mallol, C., 2019. Experimentally derived sedimentary, molecular, and isotopic characteristics of bone-fueled hearths. J. Archaeol. Method Theor 67 (6), 64.

Burke, A., 2006. Neanderthal settlement patterns in Crimea: a landscape approach. J. Anthropol. Archaeol. 25 (4), 510–523.

Canti, M.G., 2003. Aspects of the chemical and microscopic characteristics of plant ashes found in archaeological soils. Catena 54 (3), 339–361.

Canti, M.G., Linford, N., 2000. The effects of fire on archaeological soils and sediments: temperature and colour relationships. Proc. Prehist. Soc. 66, 385–395.

Carrancho, Á., Villalaín, J.J., 2011. Different mechanisms of magnetisation recorded in experimental fires: archaeomagnetic implications. Earth Planet Sci. Lett. 312 (1–2), 176–187.

Carrancho, Á., Villalaín, J.J., Angelucci, D.E., Dekkers, M.J., Vallverdú, J., Vergès, J.M., 2009. Rock-magnetic analyses as a tool to investigate archaeological fired sediments: a case study of Mirador cave (Sierra de Atapuerca, Spain). Geophys. J. Int. 179 (1), 79–96.

Carrancho, Á., Villalaín, J.J., Vergès, J.M., Vallverdú, J., 2012. Assessing post-depositional processes in archaeological cave fires through the analysis of archaeomagnetic vectors. Quat. Int. 275, 14–22.

Clark, J.L., Ligouis, B., 2010. Burned bone in the howieson's poort and post-howieson's poort middle stone age deposits at sibudu (South Africa): behavioral and taphonomic implications. J. Archaeol. Sci. 37 (10), 2650–2661.

Connolly, R., Jambrina-Enríquez, M., Herrera-Herrera, A.V., Vidal-Matutano, P., Fagoaga, A., Marquina-Blasco, R., Marin-Monfort, M.D., Ruiz-Sánchez, F.J., Laplana, C., Bailon, S., Pérez, L., Leierer, L., Hernández, C.M., Galván, B., Mallol, C., 2019. A multiproxy record of palaeoenvironmental conditions at the Middle Palaeolithic site of Abric del Pastor (Eastern Iberia). Quat. Sci. Rev. 225, 106023.

Costamagno, S., Théry-Parisot, I., Brugal, J.P., Guibert, R., 2005. Taphonomic consequences of the use of bones as fuel. Experimental data and archaeological applications. Biosphere to Lithosphere: New Studies in Vertebrate Taphonomy. Oxbow Books, Oxford, pp. 51–62.

Costamagno, S., Théry-Parisot, I., Castel, J.-C., Brugal, J.-P., 2008. Combustible ou non ? Analyse multifactorielle et modèles explicatifs sur des ossements brûlés paléolithiques. BAR International Series, 1914.

Courty, M.A., 2001. Microfacies analysis assisting archaeological stratigraphy. In: Goldberg, P., Holliday, V.T., Ferring, C.R. (Eds.), Earth Sciences and Archaeology. Springer US, Boston, MA, pp. 205–239.

Courty, M.A., Carbonell, E., Vallverdú Poch, J., Banerjee, R., 2012. Microstratigraphic and multi-analytical evidence for advanced Neanderthal pyrotechnology at Abric Romani (Capellades, Spain). Quat. Int. 247, 294–312.

Courty, M.A., Goldberg, P., Macphail, R., 1989. Soils and Micromorphology in Archaeology. In: Cambridge Manuals in Archaeology, publ ed, vol. XX. Cambridge Univ. Press, Cambridge u.a, p. 1. 344, VIII S.

Debénath, A., Dibble, H.L., 1994. Handbook of Paleolithic Typology: Lower and Middle Paleolithic of Europe. University of Pennsylvania Press.

Eckmeier, E., Wiesenberg, G.L., 2009. Short-chain n-alkanes (C16–20) in ancient soil are useful molecular markers for prehistoric biomass burning. J. Archaeol. Sci. 36 (7), 1590–1596.

Fagoaga, A., Laplana, C., Marquina-Blasco, R., Machado, J., Marin-Monfort, M.D., Crespo, V.D., Hernández, C.M., Mallol, C., Galván, B., Ruiz-Sánchez, F.J., 2019. Palaeoecological context for the extinction of the Neanderthals: a small mammal study of Stratigraphic Unit V of the El Salt site, Alcoi, eastern Spain. Palaeogeogr. Palaeoclimatol. Palaeoecol. 530, 163–175.

Fagoaga, A., Ruiz-Sánchez, F.J., Laplana, C., Blain, H.-A., Marquina, R., Marin-Monfort, M.D., Galván, B., 2017. Palaeoecological implications of Neanderthal occupation at Unit Xb of El Salt (Alcoi, eastern Spain) during MIS 3 using small mammals proxy. Quat. Int. 481, 101–112.

Farizy, C., 1994. Spatial patterning of middle paleolithic sites. J. Anthropol. Archaeol. 13 (2), 153–160.

Francés-Negro, M., Carrancho, Á., Pérez-Romero, A., Arsuaga, J.L., Carretero, J.M., Iriarte, E., 2019. Storage or cooking pots?: inferring pottery use through archaeomagnetic assessment of palaeotemperatures. J. Archaeol. Sci. 110, 104992.

Fumanal García, M.P., 1994. El yacimiento musteriense de El Salt (Alcoi, País Valenciano): rasgos geomorfológicos y climatoestratigrafía de sus registros. SAGVNTVM 27.

Gabucio, M.J., Fernández-Laso, M.C., Rosell, J., 2017. Turning a rock shelter into a home. Neanderthal use of space in Abric Romaní levels M and O. Hist. Biol. 30 (6), 743–766.

Galván, B., Hernández, C.M., Mallol, C., Machado, J., Sistiaga, A., Molina, F.J., Pérez, L., Afonso, R., Garralda, M.D., Mercier, N., Morales Pérez, J.V., Sanchis, A., Tamino, A., Gómez, J.A., Rodríguez, Á., Abreu, I., Vidal-Matutano, P., 2014a. El Salt. The last Neanderthals of the alicante mountains (Alcoy, Spain). In: Sala Ramos, R. (Ed.), Pleistocene and Holocene Hunter-Gatherers in Iberia and the Gibraltar Strait. The Current Archaeological Record. Univ. de Burgos y Fundación Atapuerca, Burgos, pp. 380–388.

Galván, B., Hernández, C.M., Mallol, C., Mercier, N., Sistiaga, A., Soler, V., 2014b. New evidence of early neanderthal disappearance in the iberian peninsula. J. Hum. Evol. 75, 16–27.

Garralda, M.D., Galván, B., Hernandez, C.M., Mallol, C., Gomez, J.A., Maureille, B., 2014. Neanderthals from el Salt (Alcoy, Spain) in the context of the latest middle

palaeolithic populations from the southeast of the iberian peninsula. J. Hum. Evol. 75, 1–15.

Goldberg, P., 2003. Some observations on middle and upper palaeolithic ashy cave and rockshelter deposits in the near east. In: Goring-Morris, A.N., Belfer-Cohen, A. (Eds.), More than Meets the Eye. Studies on Upper Palaeolithic Diversity in the Near East. Oxbow Books, Oxford.

Goldberg, P., Bar-Yosef, O., 2002. site formation processes in Kebara and Hayonim caves and their significance in levantine prehistoric caves. In: Akazawa, T., Aoki, K., Bar-Yosef, O. (Eds.), Neandertals and Modern Humans in Western Asia. Springer US, Boston, MA, pp. 107–125.

Goldberg, P., Laville, H., Meignen, L., Bar-Yosef, O., 2009a. Stratigraphy and geoarchaeological history of Kebara cave, mount carmel. In: Meignen, L., Bar-Yosef, O. (Eds.), Kebara Cave, Mt. Carmel, Israel. The Middle and Upper Paleolithic Archaeology. Part II, vol. 2. HARVARD UNIV Press, pp. 49–89.

Goldberg, P., Macphail, R.I., 2009. Practical and Theoretical Geoarchaeology. John Wiley & Sons Ltd, Hoboken, p. 478.

Goldberg, P., Miller, C.E., Schiegl, S., Ligouis, B., Berna, F., Conard, N.J., Wadley, L., 2009b. Bedding, hearths, and site maintenance in the middle stone age of sibudu cave, KwaZulu-natal, South Africa. Archaeol Anthropol Sci 1 (2), 95–122.

Groenendijk, H.A., 1987. Mesolithic hearth-pits in the Veenkoloniën (prov. Groningen, The Netherlands), defining a specific use of fire in the Mesolithic. Palaeohistoria (29).

Gualtieri, A.F., Venturelli, P., 1999. In situ study of the goethite-hematite phase transformation by real time synchrotron powder diffraction. Am. Mineral. 84 (5–6), 895–904.

Haaland, M.M., Friesem, D.E., Miller, C.E., Henshilwood, C.S., 2017. Heat-induced alteration of glauconitic minerals in the Middle Stone Age levels of Blombos Cave, South Africa: implications for evaluating site structure and burning events. J. Archaeol. Sci. 86, 81–100.

Heiri, O., Lotter, A.F., Lemcke, G., 2001. Loss on ignition as a method for estimating organic and carbonate content in sediments: reproducibility and comparability of results. J. Paleolimnol. 25 (1), 101–110.

Herrejón Lagunilla, Á., Carrancho, Á., Villalaín, J.J., Mallol, C., Hernández, C.M., 2019. An experimental approach to the preservation potential of magnetic signatures in anthropogenic fires. PloS One 14 (8), e0221592.

Herrera-Herrera, A.V., Mallol, C., 2018. Quantification of lipid biomarkers in sedimentary contexts: comparing different calibration methods. Org. Geochem. 125, 152–160.

Huisman, D.J., Niekus, M., Peeters, J., Geerts, R., Müller, A., 2019. Deciphering the complexity of a 'simple' mesolithic phenomenon: indicators for construction, use and taphonomy of pit hearths in Kampen (The Netherlands). J. Archaeol. Sci. 109, 104987.

Hunt, A., Bortolini, E. (Eds.), 2016. The Oxford Handbook of Archaeological Ceramic Analysis. Oxford University Press.

Jambrina-Enríquez, M., Herrera-Herrera, A.V., Mallol, C., 2018. Wax lipids in fresh and charred anatomical parts of the Celtis australis tree: insights on paleofire interpretation. Org. Geochem.

Jambrina-Enríquez, M., Herrera-Herrera, A.V., Rodríguez de Vera, C., Leierer, L., Connolly, R., Mallol, C., 2019. n-Alkyl nitriles and compound-specific carbon isotope analysis of lipid combustion residues from Neanderthal and experimental hearths: identifying sources of organic compounds and combustion temperatures. Quat. Sci. Rev. 222, 105899.

James, S.R., Dennell, R.W., Gilbert, A.S., Lewis, H.T., Gowlett, J.A.J., Lynch, T.F., McGrew, W.C., Peters, C.R., Pope, G.G., Stahl, A.B., 1989. Hominid use of fire in the lower and middle Pleistocene: a review of the evidence [and comments and replies]. Curr. Anthropol. 30 (1), 1–26.

Kapper, K.L., Anesin, D., Donadini, F., Angelucci, D.E., Cavulli, F., Pedrotti, A., Hirt, A. M., 2014. Linking site formation processes to magnetic properties. Rock- and archeomagnetic analysis of the combustion levels at Riparo Gaban (Italy). J. Archaeol. Sci. 41, 836–855.

Karkanas, P., Goldberg, P., 2010. Phosphatic features. Interpretation of Micromorphological Features of Soils and Regoliths. Elsevier, pp. 521–541.

Karkanas, P., Shahack-Gross, R., Ayalon, A., Bar-Matthews, M., Barkai, R., Frumkin, A., Gopher, A., Stiner, M.C., 2007. Evidence for habitual use of fire at the end of the Lower Paleolithic: site-formation processes at Qesem Cave, Israel. J. Hum. Evol. 53 (2), 197–212.

Koenigsberger, J.G., 1938. Natural residual magnetism of eruptive rocks. J. Geophys. Res. 43 (3), 299.

Koller, J., Baumer, U., Mania, D., 2001. High-tech in the middle palaeolithic: neandertal-manufactured pitch identified. Eur. J. Archaeol. 4 (3), 385–397.

Kozowyk, P.R.B., Soressi, M., Pomstra, D., Langejans, G.H.J., 2017. Experimental methods for the Palaeolithic dry distillation of birch bark: implications for the origin and development of Neandertal adhesive technology. Sci. Rep. 7 (1), 8033.

Kuhn, S.L., 1995. Mousterian Lithic Technology: an Ecological Perspective. Princeton University Press.

Kuo, L.-J., Herbert, B.E., Louchouarn, P., 2008. Can levoglucosan be used to characterize and quantify char/charcoal black carbon in environmental media? Org. Geochem. 39 (10), 1466–1478.

Leierer, L., Jambrina-Enríquez, M., Herrera-Herrera, A.V., Connolly, R., Hernández, C. M., Galván, B., Mallol, C., 2019a. Insights into the timing, intensity and natural setting of Neanderthal occupation from the geoarchaeological study of combustion structures: a micromorphological and biomarker investigation of El Salt, unit Xb, Alcoy, Spain. PloS One 14 (4), e0214955.

Leierer, L., Rodríguez, C., Mallol, C., 2019b. Micromorphological Thin Section Manufacture AMBI Lab. Universidad de La Laguna, Tenerife, Spain (protocols.io).

Løvschal, M., Fontijn, D., 2019. Directionality and axiality in the Bronze Age: cross-regional landscape perspectives on 'fire pit lines' and other pitted connections. World Archaeol. 51 (1), 140–156.

Lyman, R.L., 1994. Vertebrate Taphonomy. Cambridge University Press.

Machado, J., Molina, F.J., Hernández, C.M., Tarriño, A., Galván, B., 2016. Using lithic assemblage formation to approach middle palaeolithic settlement dynamics: el Salt stratigraphic unit X (alicante, Spain). Archaeol Anthropol Sci 1 (2), 25.

Machado, J., Pérez, L., 2015. Temporal frameworks to approach human behavior concealed in Middle Palaeolithic palimpsests: a high-resolution example from El Salt Stratigraphic Unit X (Alicante, Spain). Quat. Int. 417, 66–81.

Machado Gutiérrez, J., 2011. Contribución teórico-metodológica al análisis histórico de palimpsestos arqueológicos a partir de la producción lítica. Un ejemplo de aplicación para el Paleolítico medio en el yacimiento de El Salt (Alcoy, Alicante). Cristo Manuel Hernández Gómez, Bertila Galván Santos. Recerques del Museu d'Alcoi [en línia, pp. 33–46.

Madella, M., Jones, M.K., Goldberg, P., Goren, Y., Hovers, E., 2002. The exploitation of plant resources by Neanderthals in amud cave (Israel): the evidence from phytolith studies. J. Archaeol. Sci. 29 (7), 703–719.

Mallol, C., Henry, A., 2017. Ethnoarchaeology of paleolithic fire: methodological considerations. Curr. Anthropol. 58 (S16), S217–S229.

Mallol, C., Hernandez, C.M., Cabanes, D., Sistiaga, A., Machado, J., Rodríguez, Á., Pérez, L., Galván, B., 2013a. The black layer of Middle Palaeolithic combustion structures. Interpretation and archaeostratigraphic implications. J. Archaeol. Sci. 40 (5), 2515–2537.

Mallol, C., Hernández, C.M., Cabanes, D., Machado, J., Sistiaga, A., Pérez, L., Galván, B., 2013b. Human actions performed on simple combustion structures: an experimental approach to the study of Middle Palaeolithic fire. Quat. Int. 315, 3–15.

Mallol, C., Marlowe, F.W., Wood, B.M., Porter, C.C., 2007. Earth, wind, and fire: ethnoarchaeological signals of Hadza fires. J. Archaeol. Sci. 34 (12), 2035–2052.

Mallol, C., Mentzer, S.M., Miller, C.E., 2017. Combustion features: 31. In: Nicosia, C., Stoops, G. (Eds.), Archaeological Soil and Sediment Micromorphology. Wiley, pp. 299–330.

March, R.J., 1992. L'utilisation du bois dans les foyers préhistoriques: une approche expérimentale. Bulletin de la Société Botanique de France. Actualités Botaniques 139 (2–4), 245–253.

March, R.J., Lucquin, A., Joly, D., Ferreri, J.C., Muhieddine, M., 2014. Processes of formation and alteration of archaeological fire structures: complexity viewed in the light of experimental approaches. J. Archaeol. Method Theor 21 (1), 1–45.

Martínez-Moreno, J., Mora, R., La Torre, I. de, 2004. Methodological approach for understanding middle palaeolithic settlement dynamics at La roca dels bous (noguera, catalunya, northeast Spain. In: Conard, N.J. (Ed.), Settlement Dynamics of the Middle Paleolithic and Middle Stone Age. Tübingen Publications in Prehistory. Kerns, Tübingen.

Mathieu, C., Stoops, G., 1972. Observations pétrographiques sur la paroi d'un four à chaux carolingien. arcme 2 (1), 347–354.

Mayor, A., Hernández, C.M., Machado, J., Mallol, C., Galván, B., 2020. On identifying Palaeolithic single occupation episodes: archaeostratigraphic and technological approaches to the Neanderthal lithic record of stratigraphic unit xa of El Salt (Alcoi, eastern Iberia). Archaeol Anthropol Sci 12 (4), 25.

Meignen, L., Bar-Yosef, O., Goldberg, P., 1989. Les structures de combustion moustériennes de la grotte de Kébara (Mont Carmel, Israel). In: Olive, M., Taborin, Y. (Eds.), Nature et Fonction des Foyers Préhistoriques. Actes du Colloque International de Nemours 1987, pp. 141–146.

Meignen, L., Goldberg, P., Bar-Yosef, O., 2007. The hearths at Kebara Cave and their role in site formation processes. Cambridge, Mass. In: Bar-Yosef, O., Albert, R.M. (Eds.), Kebara Cave, Mt. Carmel, Israel. The Middle and Upper Paleolithic Archaeology. Bulletin/American School of Prehistoric Research 49. Peabody Museum of Archaeology and Ethnology Harvard Univ, pp. 91–122.

Mellars, P., 1996. The Neanderthal Legacy: an Archaeological Perspective from Western Europe. Princeton University Press, Princeton, N.J, p. 471.

Mentzer, S.M., 2012. Microarchaeological approaches to the identification and interpretation of combustion features in prehistoric archaeological sites. J. Archaeol. Method Theor 21 (3), 616–668.

Mentzer, S.M., 2017. Hearths and combustion features. In: Gilbert, A.S., Goldberg, P., Holliday, V.T., Mandel, R.D., Sternberg, R.S. (Eds.), Encyclopedia of Geoarchaeology. Encyclopedia of Earth Sciences Series. Springer Reference, Dordrecht, Heidelberg, New York, London.

Miller, C., 2011. Deposits as artifacts. TÜVA Mitteilungen (12), 91–107.

Miller, C.E., Conard, N.J., Goldberg, P., Berna, F., 2009. Dumping, sweeping and trampling: experimental micromorphological analysis of anthropogenically modified combustion features. Palethnologie 25–37.

Miller, C.E., Goldberg, P., Berna, F., 2013. Geoarchaeological investigations at diepkloof rock shelter, western cape, South Africa. J. Archaeol. Sci. 40 (9), 3432–3452.

Munsell Color (Firm), 2010. Munsell Soil Color Charts: with Genuine Munsell Color Chips. 2009 Year Revised. Munsell Color, Grand Rapids, MI, 2010.

Nicosia, C., Stoops, G. (Eds.), 2017. Archaeological Soil and Sediment Micromorphology. Wiley.

Niekus, M.J.L.T., Kozowyk, P.R.B., Langejans, G.H.J., Ngan-Tillard, D., van Keulen, H., van der Plicht, J., Cohen, K.M., van Wingerden, W., van Os, B., Smit, B.I., Amkreutz, L.W.S.W., Johansen, L., Verbaas, A., Dusseldorp, G.L., 2019. Middle paleolithic complex technology and a neandertal tar-backed tool from the Dutch north sea. Proc. Natl. Acad. Sci. U. S. A 116 (44), 22081–22087.

Olive, M., Taborin, Y. (Eds.), 1989. Nature et Fonction des Foyers Préhistoriques: Actes du Colloque International de Nemours 1987.

Paunovic, M., Culiberg, M., Turk, I., 2002. Analysis of the content of hearths from the Mousterian site of Divje babe 1 (Slovenia). Razprave IV Razreda Sazu (43), 203–218.

Pawlik, A.F., Thissen, J.P., 2011. Hafted armatures and multi-component tool design at the Micoquian site of Inden-Altdorf, Germany. J. Archaeol. Sci. 38 (7), 1699–1708.

Peeters, H., Niekus, M., 2017. Mesolithic pit hearths in the northern Netherlands function, time-depth and behavioural context. Châlons-en-Champagne Digging in the Mesolithic. Ac tes de la séance de la Société préhistorique française, 29-30 mars 2016.

Pérez, L., Machado, J., Sanchis, A., Hernández, C., Mallol, C., Galvan, B., 2020. A high temporal resolution zooarchaeological approach to neanderthal subsistence strategies on the southeastern iberian peninsula: el Salt stratigraphic unit xa (alicante, Spain). In: Cascalheira, J., Picin, A. (Eds.), Short-Term Occupations in Paleolithic Archaeology. Definition and Interpretation, first ed., Interdisciplinary Contributions to Archaeology. Springer International Publishing; Springer, Cham, Cham, pp. 237–289.

Pérez, L., Sanchis, A., Hernández, C.M., Galván, B., Sala, R., Mallol, C., 2017a. Hearths and bones: an experimental study to explore temporality in archaeological contexts based on taphonomical changes in burnt bones. J. Archaeol. Sci.: Report 11, 287–309.

Pérez, L.J., Sanchis, A., Hernández, C.M., Galván, B., 2017b. Paleoecología de Macromamíferos Aplicada a los Conjuntos zooarqueológicos de el Salt. Interaccions entre felins i humans. III Jornades d'arquezoologia, pp. 327–353.

Peters, K.E., Walters, C.C., Moldowan, J.M., 2005. The Biomarker Guide. - 1. Biomarkers and Isotopes in the Environment and Human History, vol. XVIII. Cambridge Univ. Press, Cambridge, p. 2, 471 S.

Reitz, E.J., Wing, E.S., 2008. Zooarchaeology. Cambridge University Press, Cambridge.

Rodríguez Rodríguez, A.d.C., Galván, B., Hernández, C.M., 2002. Contribución del análisis funcional en la caracterización de El Salt como un centro de intervención referencial de las poblaciones neandertalianas en los Valles de El Salt (Alicante). In: Clemente, I., Risch, R., Gibaja, J.F. (Eds.), Análisis funcional. Su aplicación al estudios de sociedades prehistóricas. Archaeopress.

Rodríguez-Cintas, Á., Cabanes, D., 2015. Phytolith and FTIR studies applied to combustion structures: the case of the middle paleolithic site of el Salt (Alcoy, alicante). Quat. Int.

Roebroeks, W., Villa, P., 2011. On the earliest evidence for habitual use of fire in Europe. Proc. Natl. Acad. Sci. Unit. States Am. 108 (13), 5209–5214.

Röpke, A., Dietl, C., 2017. Burnt soils and sediment. In: Nicosia, C., Stoops, G. (Eds.), Archaeological Soil and Sediment Micromorphology. Wiley.

Schiegl, S., Goldberg, P., Bar-Yosef, O., Weiner, S., 1996. Ash deposits in Hayonim and Kebara caves, Israel: macroscopic, microscopic and mineralogical observations, and their archaeological implications. J. Archaeol. Sci. 23 (5), 763–781.

Schiegl, S., Lev-Yadun, S., Bar-Yosef, S., El Goresy, A., Weiner, S., 1994. Siliceous aggregates from prehistoric wood ash: a major component of sediments in Kebara and Hayonim caves (Israel). Isr. J. Earth Sci. 43, 267–278.

Schiffer, M.B., Skibo, J.M., Griffitts, J.L., Hollenback, K.L., Longacre, W.A., 2001. Behavioral archaeology and the study of technology. Am. Antiq. 66 (4), 729–737.

Schmidt, P., Blessing, M., Rageot, M., Iovita, R., Pfleging, J., Nickel, K.G., Righetti, L., Tennie, C., 2019. Birch tar production does not prove Neanderthal behavioral complexity. Proc. Natl. Acad. Sci. U. S. A 116 (36), 17707–17711.

Scott, B., 2011. Becoming Neanderthals: the Earlier British Middle Palaeolithic. Oxbow Books, Oxford, Oakville, Conn, p. 234.

Shahack-Gross, R., Ayalon, A., Goldberg, P., Goren, Y., Ofek, B., Rabinovich, R., Hovers, E., 2008. Formation processes of cemented features in karstic cave sites revealed using stable oxygen and carbon isotopic analyses: a case study at middle paleolithic Amud Cave, Israel. Geoarchaeology 23 (1), 43–62.

Sievers, C., Wadley, L., 2008. Going underground: experimental carbonization of fruiting structures under hearths. J. Archaeol. Sci. 35 (11), 2909–2917.

Sistiaga, A., Mallol, C., Galván, B., Summons, R.E., 2014. The Neanderthal meal: a new perspective using faecal biomarkers. PloS One 9 (6), e101045.

Sistiaga Gutiérrez, A., March, R., Gómez, C.M.H., Santos, B.G., 2011. Aproximación desde la química orgánica al estudio de los hogares del yacimiento del Paleolítico medio de El Salt (Alicante, España), 0 Recerques del Museu d'Alcoi (20), 47–70.

Skibo, J.M., Schiffer, M.B., 2008. People and Things: A Behavioral Approach to Material Culture. Springer Science+Business Media LLC, New York, NY.

Smogorzewska, A., 2012. Fire installations in household activities. Archaeological and ethnoarchaeological study from tell arbid (North-East Syria). Paléo 38 (1), 227–247.

Speth, J.D., 2010. The paleoanthropology and archaeology of big-game hunting: protein, fat, or politics? Interdisciplinary Contributions to Archaeology. Springer, New York, p. 233.

Stacey, F.D., 1967. The Koenigsberger ratio and the nature of thermoremanence in igneous rocks. Earth Planet Sci. Lett. 2 (1), 67–68.

Stiner, M.C., Kuhn, S.L., Weiner, S., Bar-Yosef, O., 1995. Differential burning, recrystallization, and fragmentation of archaeological bone. J. Archaeol. Sci. 22 (2), 223–237.

Stoops, G., 2003. Guidelines for Analysis and Description of Soil and Regolith Thin Sections. Soil Science Soc. of America, Madison, p. 184.

Théry-Parisot, I., 2002. Fuel management (bone and wood) during the lower aurignacian in the pataud rock shelter (lower palaeolithic, les eyzies de Tayac, dordogne, France). Contribution of experimentation. J. Archaeol. Sci. 29 (12), 1415–1421.

Théry-Parisot, I., Meignen, L., 2000. Économie des combustibles (bois et lignite) dans l'abri moustérien des Canalettes [L'expérimentation à la simulation des besoins énergétiques]. Gall. Prehist. 42 (1), 45–55.

Vallverdú Poch, J., Alonso, S., Bargalló, A., Bartrolí, R., Campeny, G., Carrancho, Á., Expósito, I., Fontanals, M., Gabucio, J., Gómez, B., Prats, J.M., Sañudo, P., Solé, À., Vilalta, J., Carbonell, E., 2012. Combustion structures of archaeological level O and mousterian activity areas with use of fire at the Abric Romaní rockshelter (NE Iberian Peninsula). Quat. Int. 247, 313–324.

Vaquero, M., Pastó, I., 2001. The definition of spatial units in middle palaeolithic sites: the hearth-related assemblages. J. Archaeol. Sci. 28 (11), 1209–1220.

Vaquero, M., Vallverdu, J., Rosell, J., Pasto, I., Allue, E., 2001. Neandertal behavior at the middle palaeolithic site of abric Romani, capellades, Spain. J. Field Archaeol. 28 (1/2), 93.

Vidal-Matutano, P., 2016. Firewood and hearths: middle palaeolithic woody taxa distribution from el Salt, stratigraphic unit Xb (eastern iberia). Quat. Int.

Vidal-Matutano, P., Henry, A., Théry-Parisot, I., 2017. Dead wood gathering among Neanderthal groups: charcoal evidence from Abric del Pastor and El Salt (Eastern Iberia). J. Archaeol. Sci. 80, 109–121.

Vidal-Matutano, P., Pérez-Jordà, G., Hernández, C.M., Galván, B., 2018. Macrobotanical evidence (wood charcoal and seeds) from the Middle Palaeolithic site of El Salt, Eastern Iberia: palaeoenvironmental data and plant resources catchment areas. J Archaeol Sci Rep 19, 454–464.

Vidal-Matutano, P., Théry-Parisot, I., 2016. The Earliest Evidence of a Smoking Hearth? A Palaeoeconomical Approach from El Salt (Eastern Iberia). ESHE 6th Annual Meeting, Madrid, Spain.

Villa, P., Boscato, P., Ranaldo, F., Ronchitelli, A., 2009. Stone tools for the hunt: points with impact scars from a Middle Palaeolithic site in southern Italy. J. Archaeol. Sci. 36 (3), 850–859.

Villagran, X.S., Huisman, D.J., Mentzer, S.M., Miller, C.E., Jans, M.M., 2017. Bone and other skeletal tissues. In: Nicosia, C., Stoops, G. (Eds.), Archaeological Soil and Sediment Micromorphology. Wiley, pp. 9–38.

Villeneuve, L., Farizy, C., 1989. Les témoins de combustion du gisement moustérien de Champlost (Yonne). In: Olive, M., Taborin, Y. (Eds.), Nature et Fonction des Foyers Préhistoriques. Actes du Colloque International de Nemours 1987, pp. 135–139.

Vitezović, S., 2013. From Artefacts to Behaviour: Technological Analyses in Prehistory (Anthropologie LI).

Wadley, L., 2006. Partners in grime: results of multi-disciplinary archaeology at Sibudu Cave. South. Afr. Humanit. 18, 315–341.

Wandsnider, L., 1997. The roasted and the boiled: food composition and heat treatment with special emphasis on pit-hearth cooking. J. Anthropol. Archaeol. 16 (1), 1–48.

Wang, Q., Li, Y., Wang, Y., 2011. Optimizing the weight loss-on-ignition methodology to quantify organic and carbonate carbon of sediments from diverse sources. Environ. Monit. Assess. 174 (1–4), 241–257.

Weiner, S., Goldberg, P., Bar-Yosef, O., 2002. Three-dimensional distribution of minerals in the sediments of Hayonim cave, Israel: diagenetic processes and archaeological implications. J. Archaeol. Sci. 29 (11), 1289–1308.

Wiesenberg, G., Lehndorff, E., Schwark, L., 2009. Thermal degradation of rye and maize straw: lipid pattern changes as a function of temperature. Org. Geochem. 40 (2), 167–174.

Wragg Sykes, R.M., Coward, F., Hosfield, R., Pope, M., Wenban-Smith, F., 2015. To see a world in a hafted tool: birch pitch composite technology, cognition and memory in Neanderthals. In: Coward, F., Hosfield, R., Pope, M., Wenban-Smith, F. (Eds.), Settlement, Society and Cognition in Human Evolution. Cambridge University Press, New York, pp. 117–137.

Yravedra, J., Álvarez-Alonso, D., Estaca-Gómez, V., López-Cisneros, P., Arrizabalaga, Elorza, M., Iriarte, M.J., Pardo, J.F.J., Ses, C., Uzquiano, P., 2016. New evidence of bones used as fuel in the Gravettian level at Co?: mbre cave, northern Iberian Peninsula. Archaeol Anthropol Sci 60, 139.

Yravedra, J., Uzquiano, P., 2013. Burnt bone assemblages from El Esquilleu cave (Cantabria, Northern Spain): deliberate use for fuel or systematic disposal of organic waste? Quat. Sci. Rev. 68, 175–190.

Zerboni, A., 2011. Micromorphology reveals in situ Mesolithic living floors and archaeological features in multiphase sites in central Sudan. Geoarchaeology 26 (3), 365–391.

Zerboni, A., Massamba N'Siala, I., Biagetti, S., Di Lernia, S., 2013. Burning without slashing. Cultural and environmental implications of a traditional charcoal making technology in the central Sahara. J. Arid Environ. 98, 126–131.